EVALUATION OF PERFORATED CARBONATE CORES UNDER ACID STIMULATION

A Thesis

by

NERWING JOSE DIAZ

Submitted to the Office of Graduate Studies of
Texas A&M University
in partial fulfillment of the requirements for the degree of

MASTER OF SCIENCE

August 2010

Major Subject: Petroleum Engineering

EVALUATION OF PERFORATED CARBONATE CORES UNDER ACID STIMULATION

A Thesis

by

NERWING JOSE DIAZ

Submitted to the Office of Graduate Studies of
Texas A&M University
in partial fulfillment of the requirements for the degree of

MASTER OF SCIENCE

Approved by:

Chair of Committee,	A. Daniel Hill
Committee Members,	Hisham Nasr-El-Din
	Yuefeng Sun
Head of Department,	Stephen A. Holditch

August 2010

Major Subject: Petroleum Engineering

ABSTRACT

Evaluation of Perforated Carbonate Cores Under Acid Stimulation. (August 2010)

Nerwing Jose Diaz, B.S., Rafael Belloso Chacin University

Chair of Advisory Committee: Dr. A. Daniel Hill

Although it has been shown that clean perforation tunnels facilitate the evolution of a single, deeper-penetrating wormhole, there are no reported applications of reactive shaped charges in carbonates prior to acid stimulation. The present study was instigated to evaluate the impact of reactive charges on acid wormholing in representative carbonate cores.

A set of oil-saturated Indiana limestone and cream chalk cores have been perforated under simulated downhole conditions using either a conventional or a reactive shaped charge of equal explosive load. After CT scanning to eliminate outlying perforations affected by rock property anomalies, the set of cores were subjected to identical acid injection treatments representative of typical carbonate reservoir stimulations. Time to breakthrough and effluent chemistry were both analyzed and recorded. Finally, post-stimulation CT scans were used to evaluate wormhole morphology.

The laboratory experiments showed that reactive charges provide wider perforation tunnels with higher injectivity, which is beneficial for any type of stimulation job. Higher injectivity tunnels help to propagate more dominant and straighter wormholes resulting in less acid to break through the cores. This technology has a significant potential when perforating tight formations or heterogeneous intervals, where obtaining clean tunnels with conventional perforators is most challenging. Further research work needs to be done to evaluate if the difference in acid volume to breakthrough observed in the experiments would have a major impact in the field.

DEDICATION

This thesis is dedicated to my friends and family, especially to my wife, Cristi Navarro.

ACKNOWLEDGEMENTS

I would like to express my gratitude to Dr. A. Dan Hill for his support and patience during my research. His guidance and encouragement really helped to complete this research project. It has been a great experience.

I am very thankful to Dr. Hisham Nasr-El-Din for his guidance, advice and support during this research. His contribution to this project was a key part of it.

I also want to thank Dr. Ding Zhu for her support at the beginning of my career in this research group. Her support really helped me to start my research work.

I am also thankful to Dr. Yuefeng Sun for supporting this project and being part of my committee.

I would like to thank my friends who helped me during this experimental work. In particular, I am very thankful to Mohamed Mahmoud for running the chemical analysis of the core effluent fluids and Yanbin Zhang for teaching me everything needed to perform the acidizing experiments.

I am also very thankful to John Maldonado for all his time and help in the labs.

TABLE OF CONTENTS

CHAPTER Page

LIST OF FIGURES

Page

Page

LIST OF TABLES

Page

CHAPTER I

INTRODUCTION

1.1 Background

The lack of consistency in the techniques used in the 1920's to communicate the wellbore with the reservoir induced the development of bullet perforating equipments, which were introduced in the 1930's. This technology considerably changed the completion practices and it is still used today. According to Handren et al. (1993), the first completion performed with shaped charges was in 1949 for Gulf Oil Company, and later through-tubing perforating guns were developed and the under balanced perforating technique started being applied. Then tubing-conveyed perforating guns were introduced to the industry in the 1970's.

As can be noticed, there has been a considerable evolution in the completion techniques. Since the introduction of the perforating technology in 1932, perforations' effectiveness has been based on well productivity. Shaped charges' goal is to enhance well productivity by creating long perforations to by-pass the casing, cement and the contaminated zone resulting from drilling operations. But it is known that the stress created by the action of the jet penetrating the rock, forms a damaged zone around the perforation tunnel that is commonly called "the crushed zone". This fact has led to studies aimed at improving tunnel performance by trying to expel liner debris and crushed rock around the perforation tunnels.

It is vital to obtain clean perforation tunnels in order to achieve the desired well productivity, and a standard practice currently applied to clean perforation tunnels is the dynamic under balanced technique, the effectiveness of which depends on the near wellbore formation permeability. The limitation of this technique is the driving force required to clean the tunnels, which is not achieved in tight or low quality rock formations.

This thesis follows the style of *SPE Production & Operations.*

Obtaining clean tunnels may still not be enough to generate the required well productivity due to the formation characteristics, thus a matrix acidizing treatment is commonly carried out. Even though stimulation may be needed after perforating, the cleaning of the tunnels has significant importance at the moment of designing an acidizing job, because clean tunnels can provide higher injectivity which would lower the injection pressure needed at surface, and would also help in obtaining single and deep penetrating wormholes.

The purpose of this research study is to introduce the impact of reactive shaped charges in carbonate wormholing. The type of shaped charges tested in this research generates a secondary reaction in the perforation tunnel caused by the liner metallurgy properties and charge design. The reaction drives the expelling of liner debris and crushed zone materials, leaving a clean and undamaged tunnel. As shown by Bell et al. (2009), the reactive charge is capable of providing debris-free tunnels in sandstone formations regardless of the pressure difference, resulting in an improvement of the perforation tunnels efficiency, productivity and injectivity.

The reactive charge can be detonated in conventional gun hardware, without requiring any special handling, storage, loading or running procedures. Shot density and phasing can be the same as conventional charges. Once the explosive detonates, it converts the conical shaped charge liner into a fast-moving jet of particles, which is able to pass through the gun body, casing, cement and formation in the same way as conventional charges. Then the liner materials deposited in the perforation tunnels react exothermically, generating heat and pressure within the perforation tunnel. The overpressure breaks up and expels crushed zone materials and debris. When the rock characteristics are appropriate, fracturing of the tunnels' tip is also observed, which is an advantage to inflow performance and stimulation treatments.

1.2 Problem Summary and Objective

Perforation tunnels are the communication path between the wellbore and the reservoir in cased-hole completions. Thus the main objectives of perforating shaped charges are to

by-pass formation damage and enhance well productivity, which is achieved by maximizing penetration length and minimizing perforation damage.

Some perforating techniques have been developed to enhance well productivity, such as; static under balanced and dynamic under balanced perforating. These two techniques rely on the under balanced condition achieved during the initiation of the perforation. The difference between these two techniques is that the dynamic under balanced technique is designed to allow the high pressure wellbore and reservoir fluids flow into the empty guns and tubing, and the static underbalanced don't. Therefore, the wellbore pressure goes from underbalanced to balanced much faster when perforating using the static under balanced technique. Moreover, the dynamic underbalanced can be achieved regardless of the initial static condition. The objective of these techniques is to clean up perforation tunnels and improve their performance, by expelling the liner debris and crushed rock. But the main limitation of these techniques is that the flow needed to clean the perforation tunnels may not be achieved in tight formations.

Obtaining deep and clean perforations may still not be enough to provide the desired production rate. Therefore, a common practice is to carry out a matrix acidizing treatment in carbonate formations after completion, to create high permeability channels called wormholes, in order to increase the effective drainage area. A common way of thinking of the oil and gas industry has been that, if stimulation is required even after obtaining long and clean tunnels, the role of perforations is just to communicate the wellbore with the reservoir and the cleaning of the perforation tunnels is not considered.

It is believed that acid partially dissolves perforation debris while creating wormholes and can overcome perforation and near wellbore damage, thus tunnels' shape and perforation damage are often not considered important for the acidizing treatment. But on the other hand, Bartko et al. (2007) presented a research study in which the effect of perforation tunnels over matrix acidizing treatments is discussed, different perforating techniques were tested and it is shown that perforating design plays an important role in creating a single and deep-penetrating wormhole, and in obtaining a smaller post-treatment skin factor.

There have been research studies regarding the parameters that need to be considered when designing a matrix acidizing treatment, such as; acid injection rate, temperature, rock properties, and acid additives. Few research projects have taken into consideration the perforation tunnels.

The main objective of this research project is to study the impact of reactive shaped charges on acid wormholing in carbonate rocks. Bell et al. (2009) studied the performance of reactive shaped charges in sandstones, and it was demonstrated that this type of charge offers significant productivity improvement across a wide range of conditions.

The dynamic under balanced technique is not recommended for tight or low quality rock formations, because the under balanced pressure may not be enough to provide sufficient driving force to expel the debris from the tunnels due to the low formation permeability. But reactive charges generate a secondary reaction in the perforation tunnels, which expels the debris to leave clean and undamaged tunnels even in tight or low quality rock formations, independently from the pressure difference condition.

In this research a set of 17 core flood experiments was conducted, with 9 cores perforated with conventional shaped charges and 8 cores perforated with reactive shaped charges. The purpose of this research is to test the performance of both reactive and conventional charges and evaluate the effect of them on the matrix acidizing treatment, by comparing the flow performance of the perforated cores, CT scans before and after acidizing, acid volume to breakthrough, and wormhole geometry.

CHAPTER II

PERFORATING AND ACIDIZING FUNDAMENTALS

2.1 Perforating Fundamentals

The main objective of modern perforating techniques is to establish an effective flow communication between a cased wellbore and a reservoir. Perforating guns are very commonly used nowadays to obtain that communication path. Many years ago bullet perforating was the number one technique to open up cased and cemented sections to flow, but this technique plugs the tip of the perforation tunnels resulting in a flow restriction. Therefore, shaped charges (**Fig. 1**) were designed to improve the perforating technique and are the ones commonly used today.

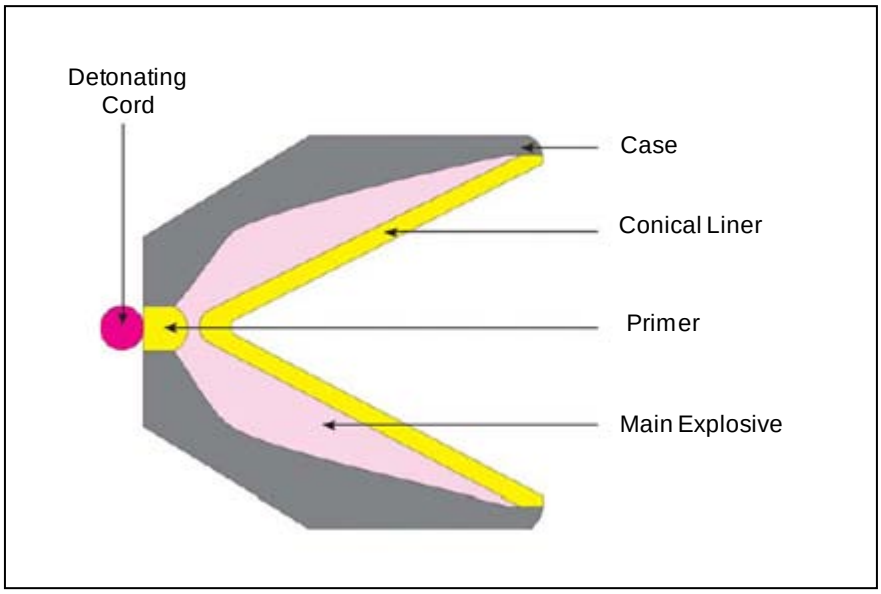

Fig. 1—Schematic of shaped charge.

Modern well perforating guns are attached either to a wire line or coiled tubing. **Fig. 2** shows the schematic of a gun system with shaped charges, which shows the main components of the system and the detonation sequence. The energy resulting from the detonation is directed by the conical case. The charge liner plays an important role, since

this is the part which collapses and emerges at a high velocity, creating a jet of metal particles.

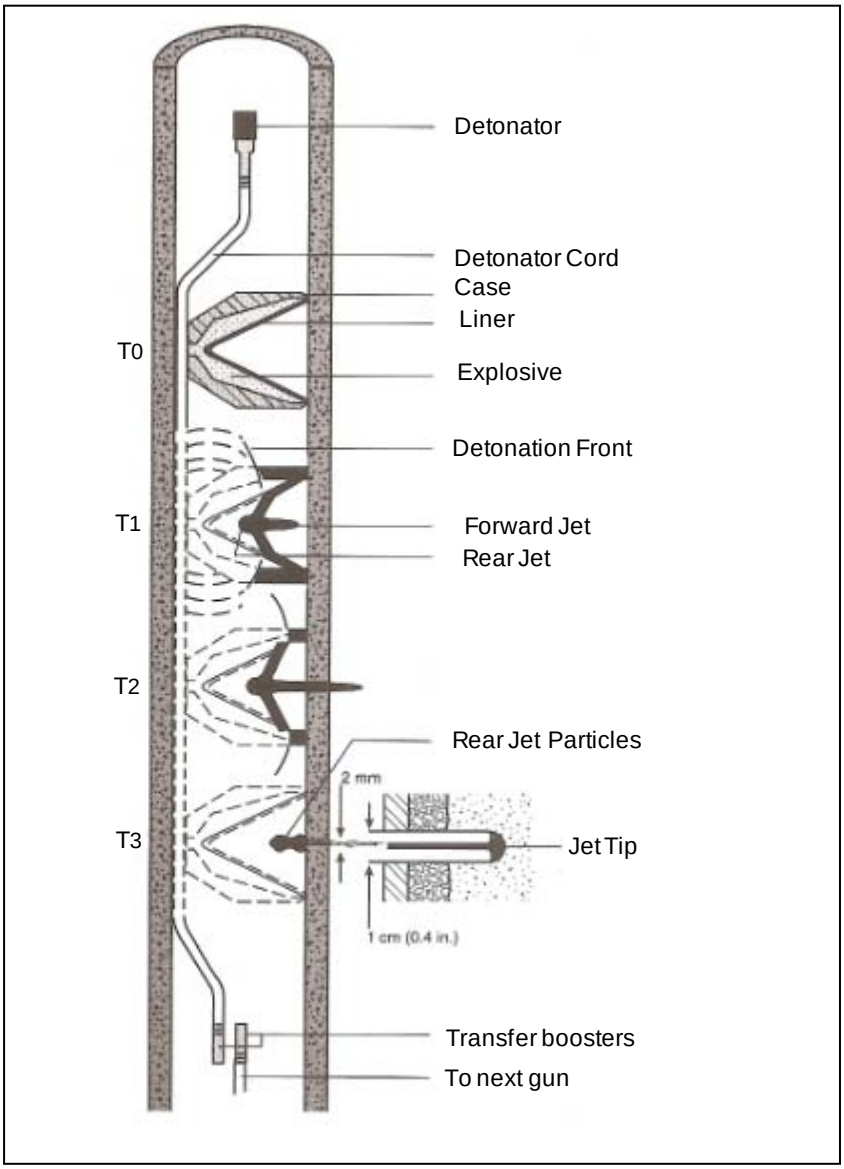

Fig. 2—Perforating gun and detonation sequence (Economides et al. 1994).

The pulse moves out at around 30,000 ft/sec (20,000 miles/h) and generates pressures between 5 and 15 million psia (Bellarby, 2009). The high pressure deforms the wellbore casing and crushes the cement and formation. The wellbore material is not

destroyed or vaporized during this process, so debris (liner material and crushed rock) is created, which should be expelled before the perforation tunnels can perform efficiently.

The diameter and length of perforation tunnels are dependent on the gun type, reservoir characteristics, and formation stresses. Very commonly, perforation tunnels are created with a diameter between 0.25 to 0.4 in. and a length between 6 and 12 in. (Economides et al. 1994).

The productivity of a well is dependent on several factors, such as the flow restriction (pressure drop) in the near wellbore area. This pressure drop is taken into consideration within the "Skin factor". Perforations are known for creating formation damage, which comes from the crushed rock around the perforation tunnels and from the liner debris remaining in the tunnels. **Fig. 3** shows the schematic of a perforation with these characteristics.

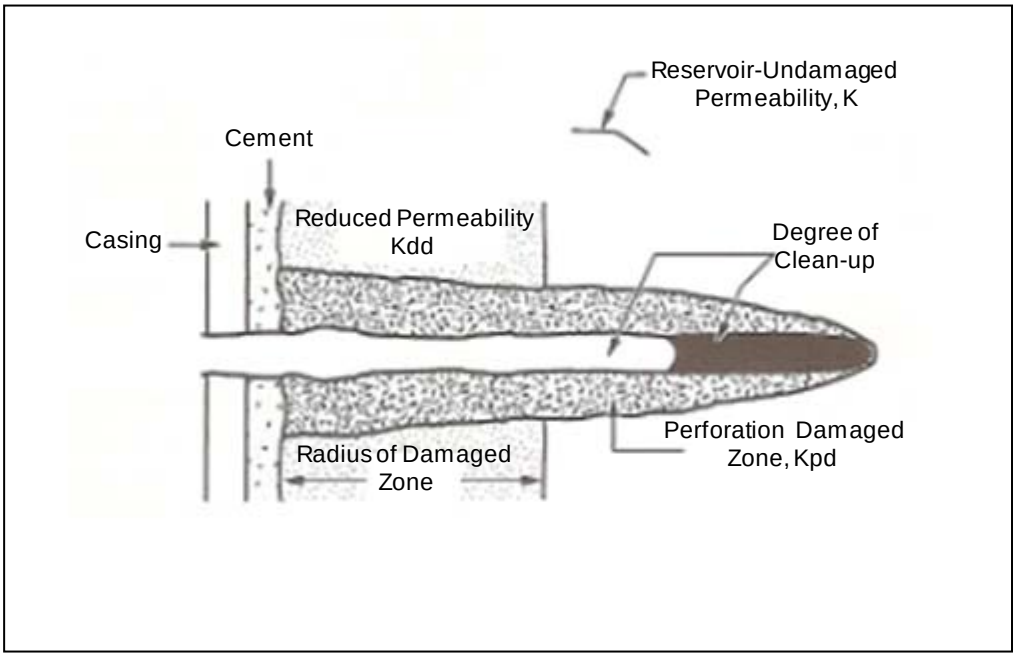

Fig. 3—Sources of pressure drop in a perforated system (Bell et al. 1995).

The perforation skin is dominated by three mayor components, which are the perforation geometry, formation characteristics, and perforating environment. Perforation geometry is defined by the shot density (number of perforation tunnels per

foot), depth of penetration, phasing (angle between perforations), and perforation tunnel diameter. The formation properties should be considered in addition to the geometric factors, because the type of formation and in-situ stress conditions strongly affect the perforation length and level of damage.

It is known that drilling and cementing operations create a zone of reduced permeability around the wellbore, resulting from mud and cement filtrate or solids invasion. This reduced permeability zone negatively affects the perforating environment which must be considered for the perforating design. Perforation tunnels should be designed to be long enough to bypass this zone in order to improve productivity and injectivity.

Perforating is very commonly carried out underbalanced (static or dynamic) in order to try to clean up the tunnels, by expelling the liner debris into the wellbore and minimizing the crushed rock around the perforations. Most of the liner debris is expelled by the transient flow with a sufficient underbalanced pressure, and then steady state flow gradually reduces the perforation damage. The underbalanced condition is essential for this practice. Insufficient underbalanced pressure would result in inadequate cleanup. On the other hand, a too high underbalanced pressure may cause mechanical failure of the formation and movement of fines. The efficiency of this perforating technique is mainly dependent on the formation permeability and reservoir fluids properties, thus the efficiency of this technique is very limited in tight or low quality rock formations.

2.2 Overview of Early and Latest Perforating Techniques

Perforating techniques have been improved to try to optimize perforations efficiency, which is the main topic on this section. Mechanical perforators were the earliest methods mostly used, such as the perforating knife shown in **Fig. 4** (Bell et all. 1995). The knife was tripped down open and an upward pull on the pipe pushed the knife through the casing wall, this practice was highly time consuming and expensive. Furthermore, this tool was not efficient to reach a significant distance to bypass the cement.

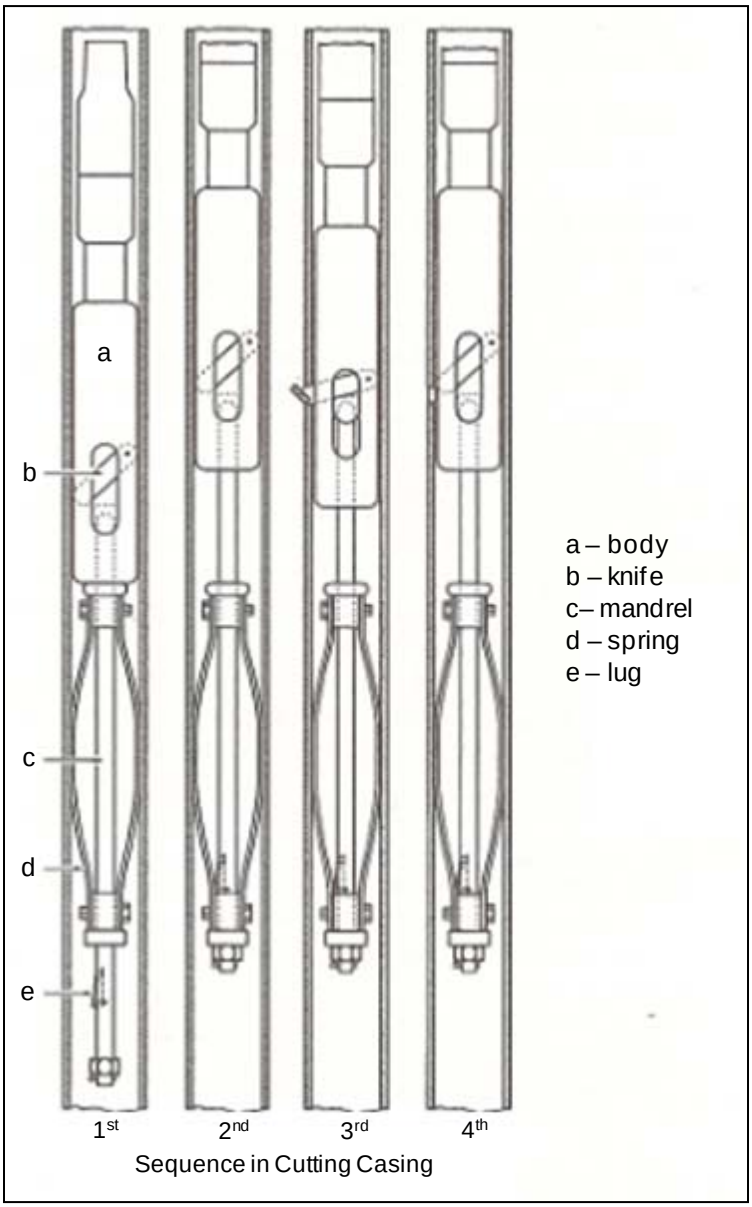

Fig. 4—Mechanical knife perforator (Bell et al. 1995).

Later bullet guns were designed for perforation, which were operated through an electric wire line. This type of tool used propellant charges to shoot bullets through the casing and cement. This technique was not very efficient in terms of providing an adequate flow path, because a bullet was literally shot into the formation, plugging up the tip of the perforation tunnel (**Fig. 5**).

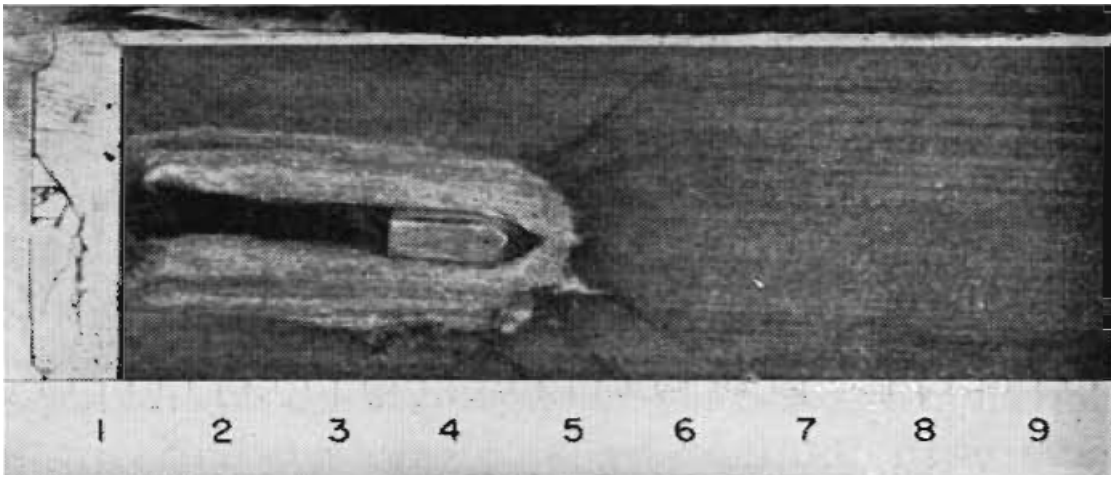

Fig. 5—Bullet gun perforating (Allen and Worzel. 1956).

Since there was a lack of consistency and reliability in the techniques used at that time, perforating shaped charges were designed. The first commercial job was carried out in 1949, through a hollow steel carrier. Most of the early jobs were carried out over balanced at that time. Later through-tubing perforating guns were designed which introduced the concepts of underbalanced and dynamic underbalanced perforating.

As discussed before, liner debris from the shaped charges remain in the perforation tunnels after deployment, and they should be expelled in order to provide an efficient flow path and increase productivity. Underbalanced and dynamic underbalanced perforating is commonly used nowadays to clean up the perforation tunnels, when the reservoir properties are adequate to do so.

Another perforating technique currently applied to increase productivity is the extreme overbalanced pressure perforating. According to Handren et al. (1993), fractures around the perforation wall are created due to the stress generated by the action of the jet penetrating the rock. The extreme overbalanced technique relies on this fact by applying pressure immediately after these fractures are created in order to extend their length.

A new type of shaped charge was introduced to the industry in 2007 by Langan, T. et al., which is discussed and evaluated in this research work. This class of shaped charge generates a secondary reaction immediately after deployment. This exothermic reaction is driven by the liner metallurgic properties, resulting in an increase of

temperature and pressure in the perforation tunnels. The increase in pressure causes the expelling of the liner debris and crushed rock materials into the wellbore. It is believed that this technology is capable of providing clean tunnels, regardless of the pressure difference condition.

2.3 Matrix Acidizing Fundamentals in Carbonate Reservoirs

In carbonate matrix acidizing treatments, acid (very commonly hydrochloric acid) is injected at pressures below the formation fracture pressure. The objective of this stimulation treatment is to achieve radial acid penetration in the formation, in order to increase the near wellbore formation permeability. After acid injection, an after-flush of water or hydrocarbon is carried out to clear the acid from the tubulars. Corrosion inhibitors are usually added to the acid mixture to protect the wellbore tubulars, and other additives are used such as, iron chelating agents, antisludge agents, mutual solvents, and others, depending on the specific requirements of the formation and wellbore.

Matrix acidizing enhances well productivity when near-wellbore damage is present, but on the other hand; it would not provide much benefit in undamaged wells (low damage skin factors). Therefore, matrix acidizing treatments are generally carried out in wells with a high skin effect that does not result from mechanical aspects of the completion. **Fig. 6** shows an example of a typical productivity improvement when removing damage by applying a matrix acidizing treatment.

The chemical reaction between hydrochloric acid and carbonate formations is governed by the following expressions;

Calcite:

$$2HCl + CaCO_3 \rightarrow CaCl_2 + CO_2 + H_2O \quad \text{(1)}$$

Dolomite:

$$4HCl + CaMg(CO_3)_2 \rightarrow CaCl_2 + MgCl_2 + 2CO_2 + 2H_2O \quad \text{(2)}$$

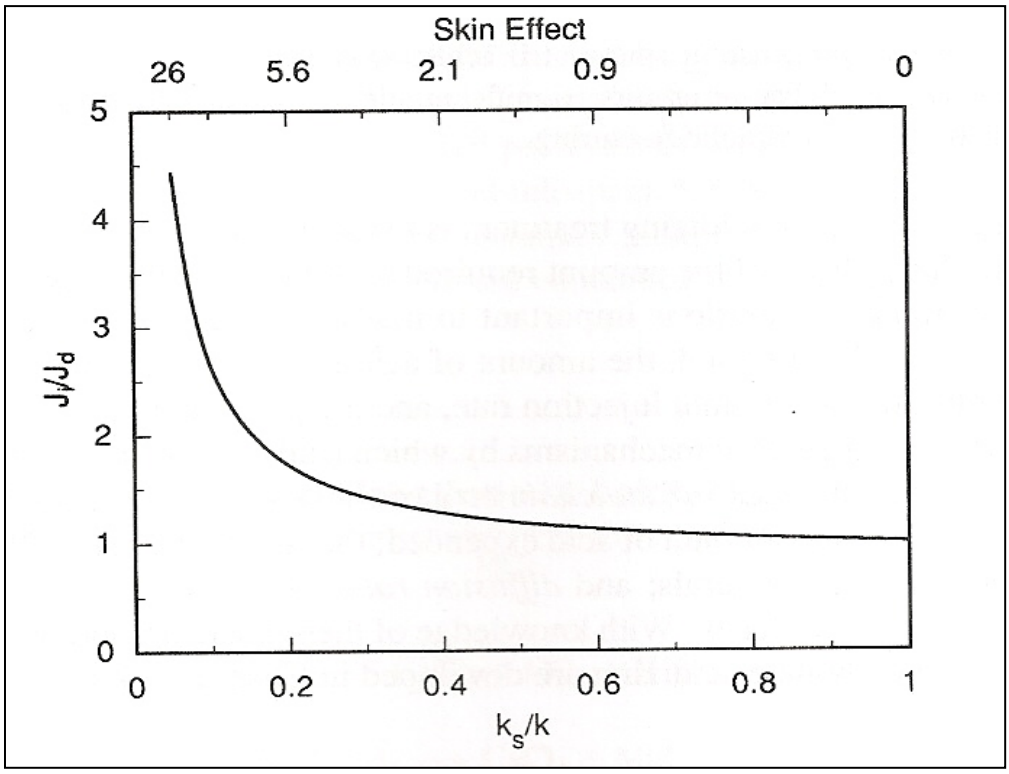

Fig. 6—Productivity improvement from acidizing (Economides et al. 1994).

The dissolving power is a more practical way of expressing the stoichiometry, introduced by Williams et al. (1979). This expression represents the amount of mineral that can be consumed by a given amount of acid on a mass or volume basis (Economides et al. 1994). The gravimetric dissolving power is the mineral consumed by a certain amount of acid on mass basis, and it is defined as;

$$\beta = \frac{v_{mineral} MW_{mineral}}{v_{acid} MW_{acid}} = \frac{lbmCaCO_3}{lbmHCL} \quad \text{..... (3)}$$

And the volumetric dissolving power is the mineral dissolved by a certain amount of acid on volume basis, which is expressed as;

$$X_{wt\%} = \beta \frac{\rho_{acid\ solution}}{\rho_{mineral}} = \frac{ft^3 CaCO_3}{ft^3 wt\%HCL} \quad \text{..... (4)}$$

The reaction between hydrochloric acid and carbonates are defined as heterogeneous, since it consists of a reaction of two different phases, the aqueous phase which is the acid and the solid minerals. The overall rate of mineral dissolution or acid

consumption depends on two factors, which are the transport rate of acid to the mineral surface and the reaction rate of the acid on the mineral surface. One of these two phenomenons is much faster than the other depending on the type of species reacting, thus the fast process is ignored because it occurs in a fraction of the time that takes the slow process to occur. For example, the HCl-$CaCO_3$ reaction is very fast, thus the overall rate of this reaction is controlled by the rate of acid transport.

When acid is injected to carbonate formations at pressures below the fracture pressure, acid follows the path of highest permeability or less resistance. The reaction in these flow paths causes the creation of large permeability channels which are called wormholes. Wormholes form in a dissolution process when the large pores grow at a rate substantially higher than the rate at which smaller pores grow, so that a large pore receives an increasingly larger proportion of the dissolving fluid, eventually becoming a wormhole (Economides et al. 1994). Wormhole formation is dependent on the chemical reaction rate of the acid with the rock, and high reaction rates normally tend to help the wormhole creation.

Flow rate and acid flux also affect wormholes propagation. **Fig. 7** shows the results obtained in a study carried out by Wang et al. (1993), in which the concept of "optimal injection rate" is discussed. This study is based on carbonate core flood experiments. It can be observed that as the acid injection rate increases the volume of acid needed to breakthrough decreases, a minimum acid volume to breakthrough is reached at the optimum injection rate, and then the acid volume to breakthrough starts slowly increasing as the injection rate increases.

This behavior can be explained by the type of dissolution patterns being created. At low injection rates, the acid is spent reacting with the rock face and wormholes walls which results in a very high volume to break through. At the intermediate rate, a single wormhole can be formed that break through the core consuming less acid. However, when the injection rate is increased at values higher than the optimum, highly ramified wormholes are created rather than single dominant wormholes, and the creation of multiple wormhole branches requires more acid to propagate a certain distance.

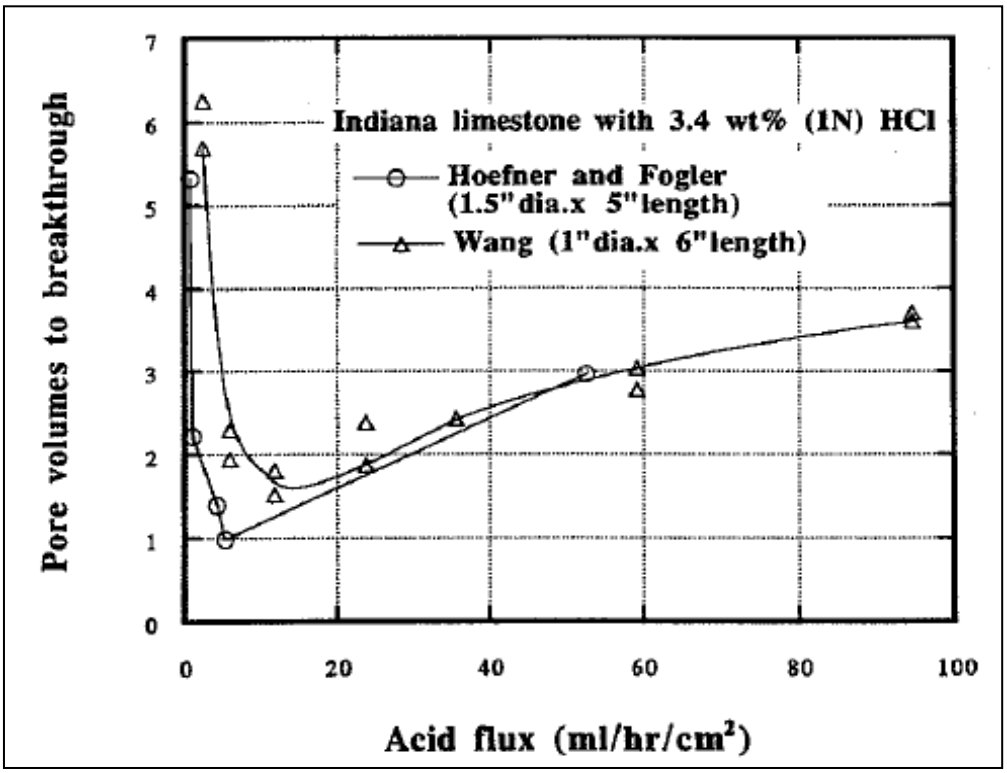

Fig. 7—Optimum injection rate (Economides et al. 1994).

There are other parameters that affect the propagation of wormholes which should be considered at the moment of designing an acidizing job, such as rock mineralogy, temperature, acid concentration, and additives. This is the reason why experimental simulations and the simulation through mathematical models are highly recommended while designing an acidizing job, since different formations and acid mixtures would provide different results.

CHAPTER III

EXPERIMENTAL PROCEDURE AND PARAMETERS

3.1 Preparation and Perforating of Cores

This research work is based on seventeen core flood experiments, from which eleven were carried out with Indiana limestone cores and six with cream chalk cores. In order to compare the results obtained from the experiments, the cores were cut from the same block of rock, which provides the certainty that the rocks have similar properties.

After selecting the type of rock and cutting the core samples, they are saturated by placing the cores in a container connected to a vacuum pump. The vacuum pump is used to force the fluid to go into the pore space. Oil mineral spirits was used for saturation and to run the experiments. Its density and viscosity are shown in **Fig. 8**.

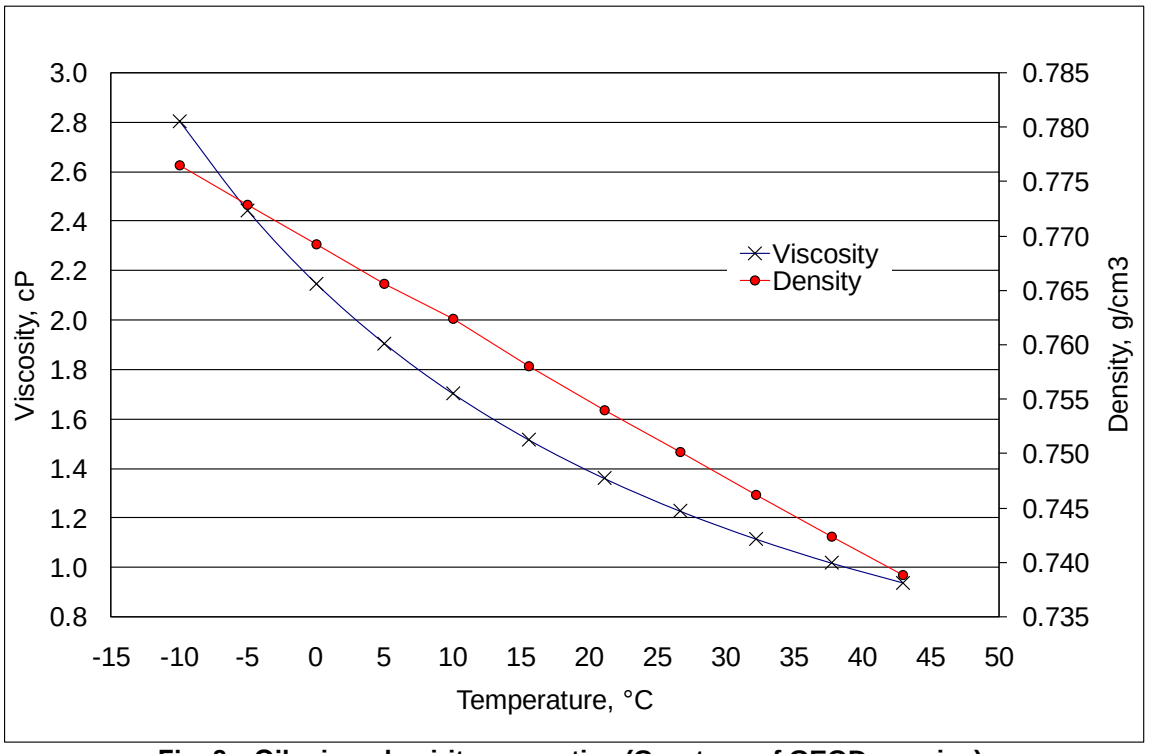

Fig. 8—Oil mineral spirits properties (Courtesy of GEODynamics).

Once the core is saturated, the weight of the wet rock is measured so that the pore volume and porosity of the core can be calculated. **Fig. 9** shows the picture of one Indiana limestone core sample (right side) and one cream chalk core sample (left side), which are 20 inches long and 4 inches in diameter.

Fig. 9—Carbonate core samples (4 inches in diameter and 20 inches long).

The core is then loaded into the pressure vessel to carry out the perforating (**Fig. 10**). The simulated wellbore is filled with fluid, and then the pore pressure is applied at the same time the overburden pressure is applied. Once the desired wellbore and pore pressure are reached, the charge is detonated. Later the wellbore and pore pressure are

allowed to equalize, and the overburden pressure is slowly reduced at the same rate the pore pressure is released. When the wellbore and pore pressure reach atmospheric pressure, the wellbore is opened to retrieve the gun.

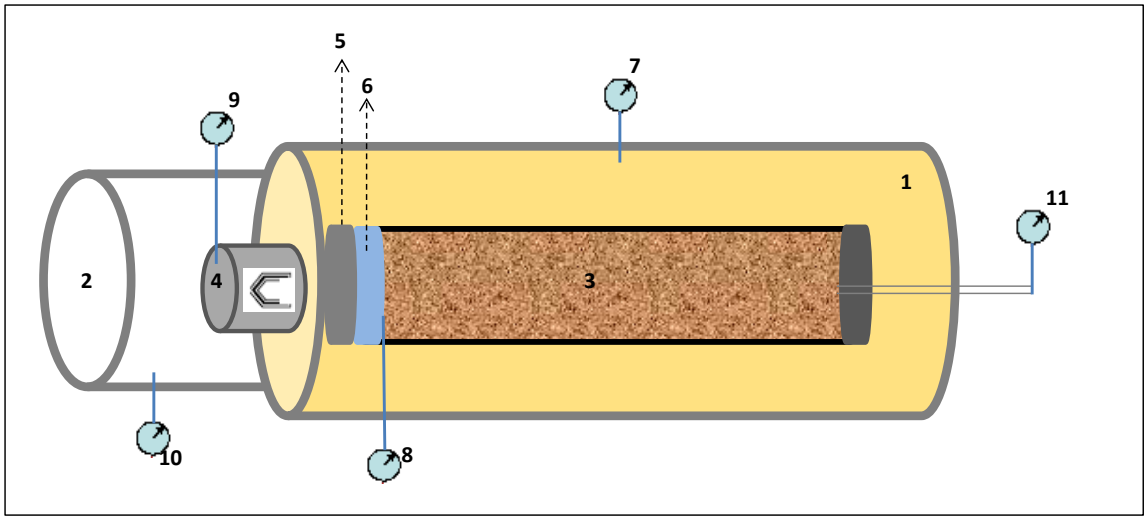

Fig. 10—Perforating set-up. (1) Confining chamber (2) Simulated wellbore (3) Core sample (4) Gun with shaped charge (5) Simulated casing (6) Simulated cement (7) Pressure transducer (8) Pressure transducer for core inlet pressure (9) Pressure transducer for gun pressure (10) Pressure transducer for wellbore pressure (11) Pressure transducer for reservoir pressure.

3.2 CT Scanning of Cores

After perforating the core samples, they are characterized by using CT scanning. This step is carried out to identify geometric anomalies and fracturing caused by variations in the rock targets, and also to evaluate the original condition of the perforation tunnels. The images of the scans are generated from a set of CT numbers, which correspond to the density of the materials scanned. High CT numbers represent materials with high density and small CT numbers represent materials with low density. Thus the length and diameter of the perforation tunnels can be obtained from the images, since the range of CT numbers in the perforation tunnel zone is different from the range of CT numbers of the rock. The presence of debris can be identified as well, since the rage of CT numbers of the rock is different from the rage of CT numbers of the liner materials.

The CT scanner is set to take a picture of the core every 3 mm. **Fig. 11** shows an example of a perforated core image. It can be observed on this picture that there are different colors in the core. The color green represents the matrix, the color blue represents the perforation tunnel free of debris, and the pink or red color represents the debris inside the perforation tunnel. At the bottom of the figure there is a legend, which indicates the CT number rage for every color.

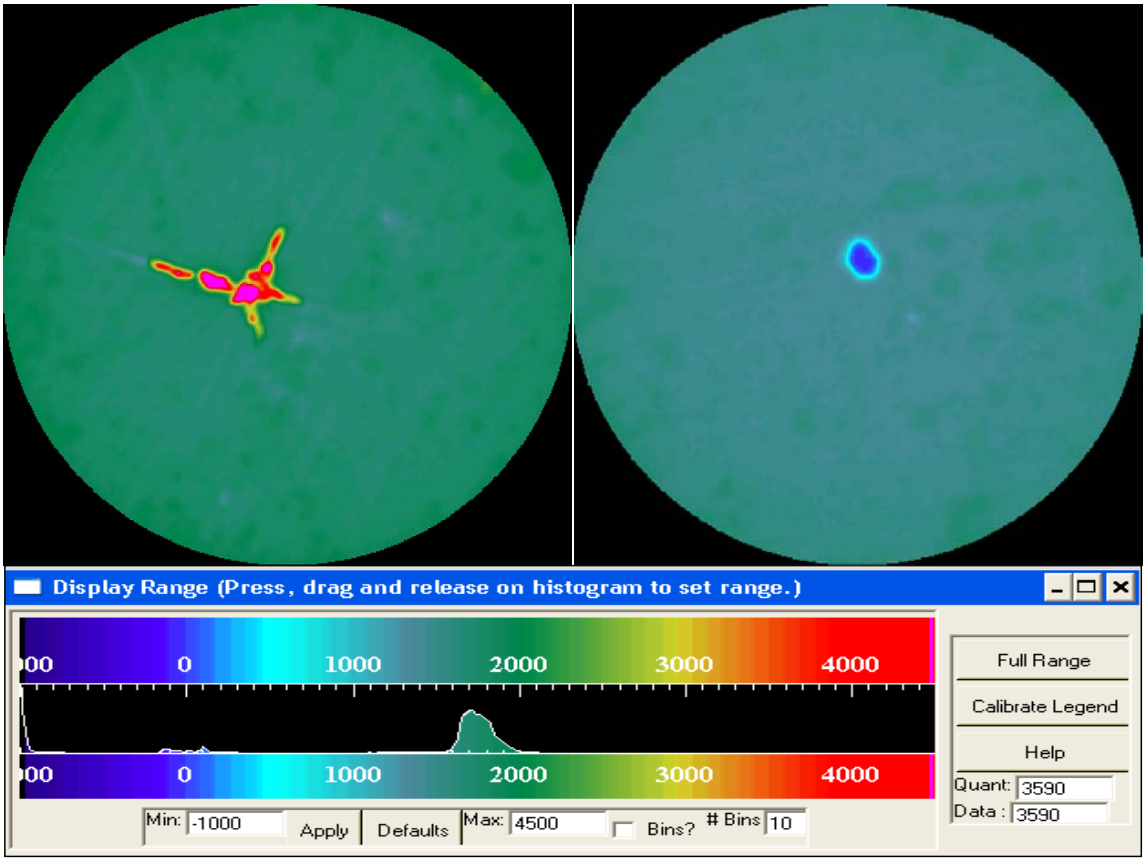

Fig. 11—2D CT images of perforated cores.

Fig. 12 shows the image that is obtained after scanning the entire core. Every slide can be studied independently to determine the presence of debris and the dimensions of the perforation tunnel at any part of the core. This set of slides is then converted into a three dimensional picture, which is shown in **Fig. 13**. The three dimensional image is used to identify the flow path of acid and observe the wormholes.

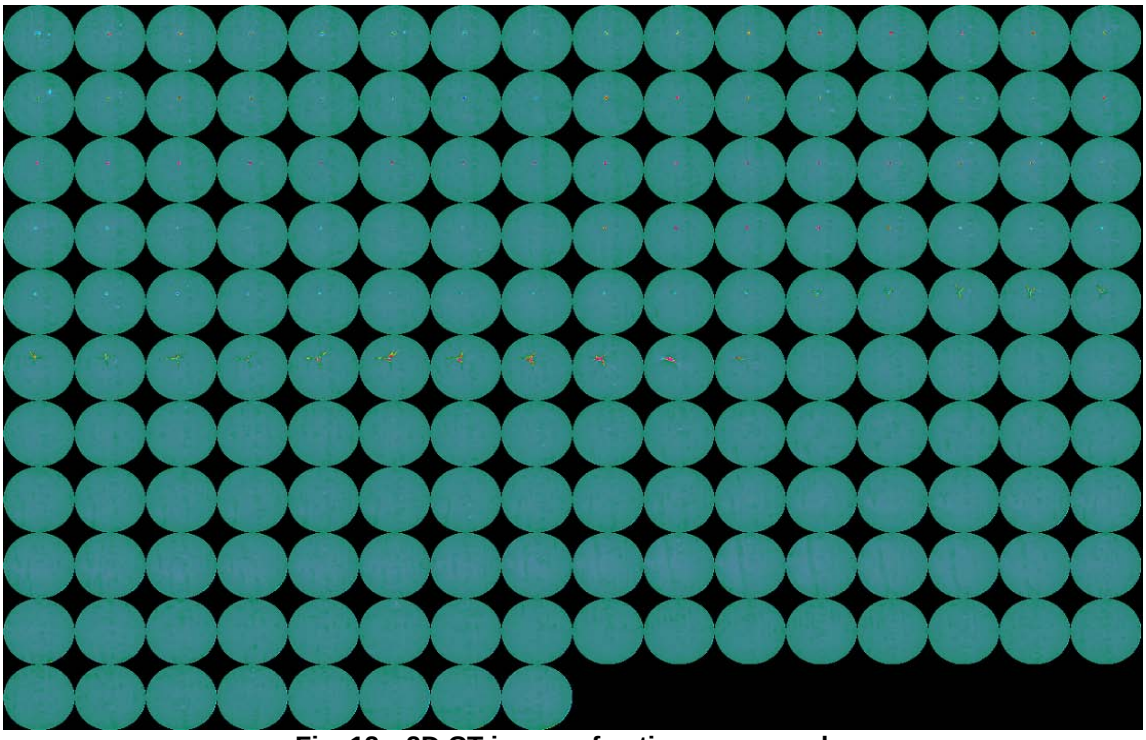

Fig. 12—2D CT image of entire core sample.

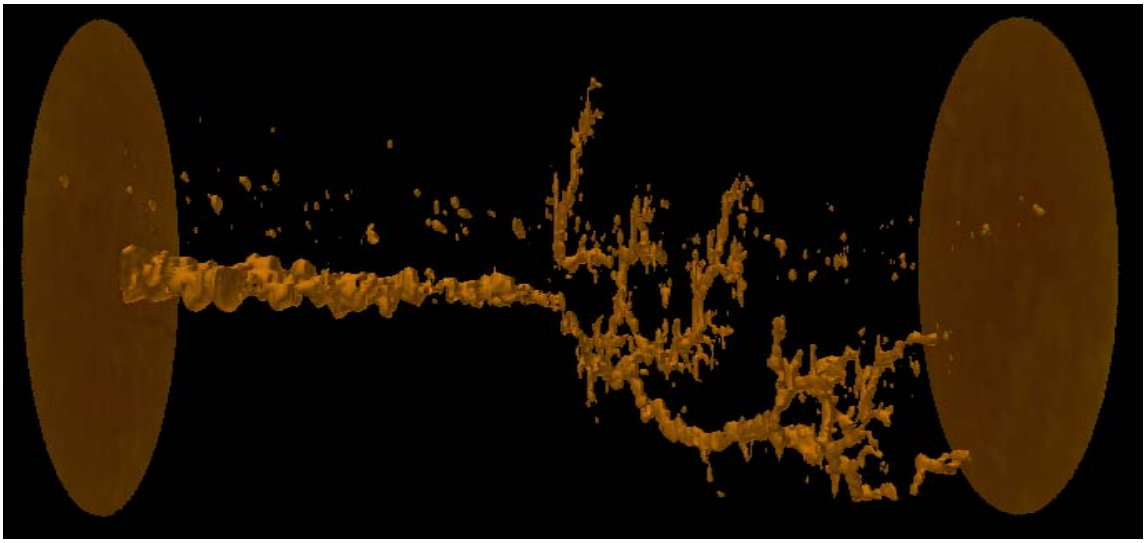

Fig. 13—3D CT image of entire core sample.

3.3 Acidizing of Perforated Cores

The core is first placed in the core holder which is described in the following chapter. The outlet pressure is set to be 1000 psi to ensure that the pressure in the entire system is

above 1000 psi, in order to keep the CO_2 that results from the reaction between HCL and $CaCO_3$) in solution while acid is injected.

Once the apparatus is set, the flow performance of the core is then evaluated by pumping mineral oil through the core sample at a 10 cm^3/min rate until steady state flow is reached. The injectivity of the core is measured and the results are presented and explained in Chapter V. The pressure is recorded while running the experiment which gives the advantage of monitoring the pressure accurately in real time. **Fig. 14** shows a typical pressure response during a core flood experiment, from which can be observed that steady state flow is reached at 368 psi pressure difference.

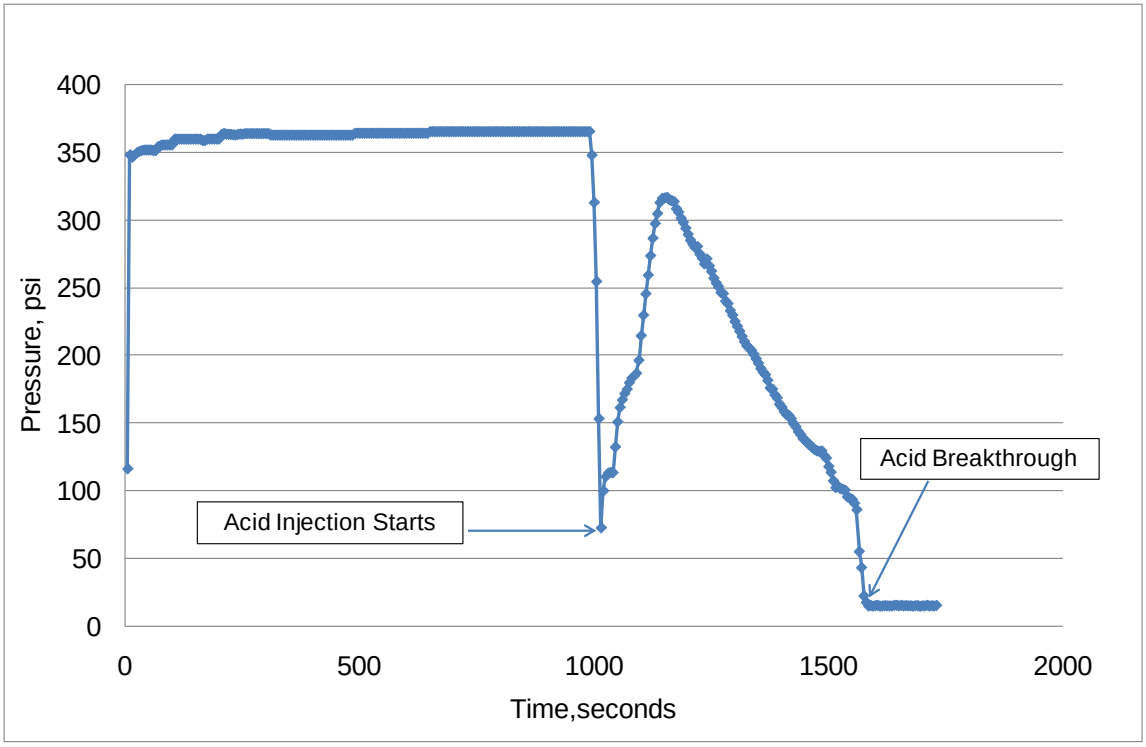

Fig. 14—Typical pressure response during a core flood experiment.

This step is carried out to compare the flow performance of the cores perforated with conventional and reactive shaped charges before acidizing. Since the core samples have similar properties, the flow performance of the cores is affected just by the efficiency of the perforation tunnels. After reaching steady state flow, there is a pressure

decline due to the switch from oil to acid (the pump has to be stopped to close and open some valves). Later pressure starts increasing as acid is injected, a peak is reached and then pressure decreases as the acid reacts with the core and wormholes propagate until acid breaks through the core. Acid volume to breakthrough is measured to later calculate the pore volumes needed to breakthrough, this is done by calculating the pore volume from the tip of the perforation to the end of the core, which is the area that acid has to flow through. Pore volume needed to breakthrough is just the ration of acid volume divided by the core pore volume.

After acidizing, a flow back is carried out through the core by pumping oil in the opposite direction. This step is carried out to simulate a real stimulation treatment in the field. This allows to identify the presence of liner debris remaining in the perforation tunnel after acidizing. If liner debris remain in the perforation tunnel after acidizing, some of it would be observed coming out from the flow lines.

3.4 Compositional Analysis of Effluent Samples

Fluid samples are collected throughout the core flood experiment, and the equipment for collection and analysis are described in the following chapter. The collection of samples helps to confirm the exact time that acid breaks through the core, since acid would be observed at the outlet of the apparatus once acid breaks through the core. This step is also carried out to perform a compositional analysis of the effluent fluids and evaluate their behavior, by measuring the acid and calcium concentration. The acid (HCL) concentration is measured with the acid based titration method, by using an autotitrator and the calcium concentration is measured with the atomic absorbance technique. The data of the samples allows the verification of the exact time that acid breaks through the core, which is then used to compute the volume of acid used to breakthrough.

Since there is not an accurate means to calculate the amount of debris from the CT scan images, the measurement of heavy metals concentration in the fluid samples could provide a better understanding of the cleaning efficiency.

CHAPTER IV

EXPERIMENTAL APPARATUS

4.1 Equipment for Core Samples Perforation

As discussed previously, the perforating of the core samples is performed in a pressure vessel (Fig. 10). This apparatus is comprised of two chambers, one chamber which simulates the wellbore with a simulated gun, and another chamber holds the core to simulate the reservoir. This apparatus allows the perforation of cores under different pressure conditions, such as balanced, underbalanced or overbalanced. This permits the simulation of different real field scenarios.

The core sample is held inside a rubber sleeve that is pressurized to simulate the overburden pressure, which ensures that the fluids flow across the core. Both a metal plate and a cement plate are placed in the inlet of the core, to simulate the casing and cement in a well.

The perforating vessel is controlled from a separate room where the pressure is monitored by using pressure transducers connected to a data acquisition system inside the control room. The detonation of the gun is carried out from the control room as well, to ensure that the operators are located at a safe distance from the perforating apparatus.

4.2 CT Scanner

Computerized Tomography (CT) is an imaging technique which was invented for medical purposes, but the CT scanner is now being used for a wide variety of applications such as the study of flow in porous media, since it allows the determination of rock properties like porosity and density. CT is an imaging technique that uses X-Ray technology to reconstruct a three-dimensional object from a series of cross-sectional images made along an axis. When an object such as a core sample is scanned, beams from an X-Ray source penetrate the core, and the rays that come out through the core are captured by a set of detectors. **Fig. 15** shows the scanner used for this experimental study. This is a Universal HD200 scanner. It has a 50 cm maximum diameter and a

maximum scan speed of 2 sec. It has an automatic sample table with a travel precision of 0.1 mm. This equipment is used to create three dimensional images which allow the visualization of the perforation tunnels and wormholes in the core samples.

Fig. 15—CT Scanner (Courtesy of Harold Vance, Department of Petroleum Engineering, Texas A&M University).

4.3 Equipment for Flow Performance Evaluation and Acidizing

As shown in **Fig. 16**, the apparatus for the core flood experiments is comprised of several elements which are described in this section. The core holder is made of Hastelloy, which is an acid resistant material. **Fig. 17** shows the main components of the core holder. **Fig. 17-A** is the main body of the core holder, which has a rubber sleeve in the inside. The annulus space between the main body and the sleeve is filled with oil to simulate the overburden pressure during the experiment. **Fig. 17-B** shows the inlet cap with three tubes. One tube is connected to the pressure transducers, the tube located in the middle is connected to the fluid containers, because this is the line used for fluid injection, and the third tube is kept closed during the fluids injection, but it is opened after acidizing and used as an outlet line to flow back, which is done in the field after an stimulation job. **Fig. 17-C** shows a holder which is used to keep the inlet cap in place. The outlet cap is comprised of three elements (**Fig. 17-D, 17-E and 17-F**) that together

are used to tighten the outlet of the apparatus to make sure the core sample is in contact with the inlet and outlet cap.

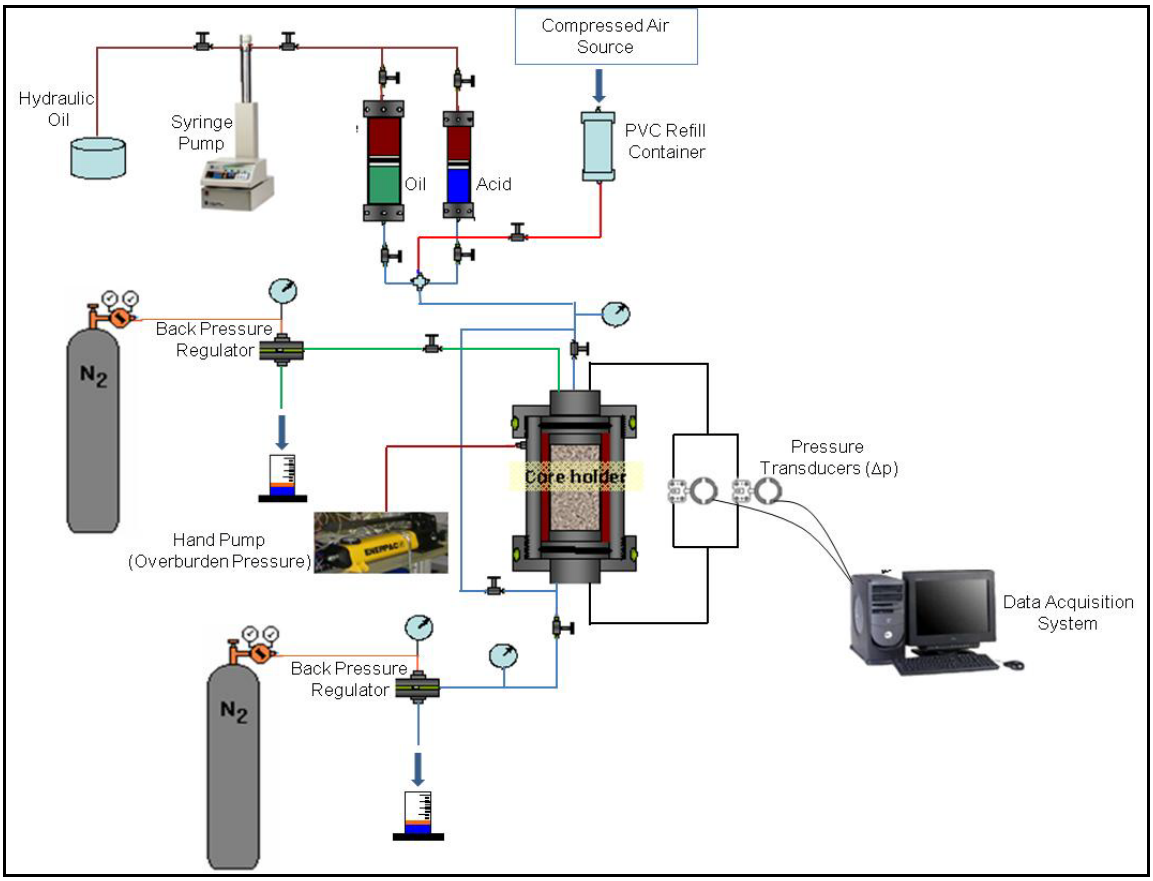

Fig. 16—Apparatus for core flood experiments.

A syringe pump is used for the fluids injection. As shown in the schematic (Fig. 16), this pump injects oil to the piston containers which are filled with oil and acid respectively. Pressure drives the movement of the piston which at the same time drives the injection of the fluids from the containers. The pump has a volume capacity of 1000 ml and it has a control panel which allows the monitoring of the pumping time and volume of oil remaining in the pump during the experiment. This panel also permits the control of both the pumping flow rate and pressure.

The set-up also has a couple of back pressure regulators (Fig. 16). One regulator is located at the outlet of the system, and it is set to 1000 psi during the entire

experiment. This is done to make sure that the pressure in the entire system is above 1000 psi, which ensures that the CO_2 resulting from the interaction between the acid and the rock remains in solution. The second back pressure regulator is connected to one of the tubes located in the inlet cap. As mentioned before, this tube is used for the flow back that is carried out after acidizing, thus the pressure regulator is set to 1000 psi as well during the flow back for the same reason, which is to keep CO_2 in solution during the flow back to have single phase flow.

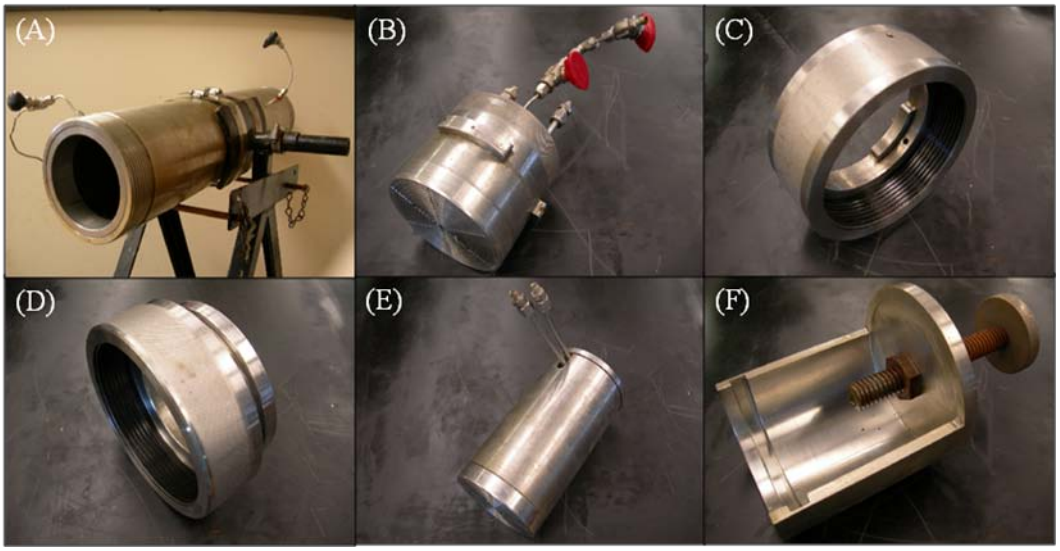

Fig. 17—Core holder.

As discussed previously, the annulus space between the main body of the core holder and the rubber sleeve is filled with oil to simulate the overburden pressure. This oil is pumped with a hydraulic ENERPAC pump (**Fig. 18**), which has a volume capacity of 55 cubic inches and is capable of holding pressures up to 10,000 psi. This pump works with conventional motor oil.

The pressure transducers shown in **Fig. 19** are connected to the inlet and outlet of the core holder, which allows the measurement of pressure difference across the core. The transducers are connected at the same time to a data acquisition system that permits the monitoring of pressure in real time. LabView is used to display and record the

pressure. This program records pressure difference every 5 seconds and plots the results while recording the data.

Fig. 18—Hydraulic hand pump.

Fig. 19—Pressure transducer.

Effluent fluid samples are collected during the core flood experiment. This is done with the help of a Gilson automatic collector which is shown in **Fig. 20**. These collectors are set to collect samples every certain period of time, which depends on the

volume capacity of the tubes and the flow rate. These samples are then placed in plastic tubes and sealed properly, to later allow for compositional analysis.

Fig. 20—Automatic fluid samples collector.

4.4 Equipment for Compositional Analysis of Effluent Samples

The acid concentration is measured using the acid base titration method, with the help of an autotitrator (**Fig. 21**).

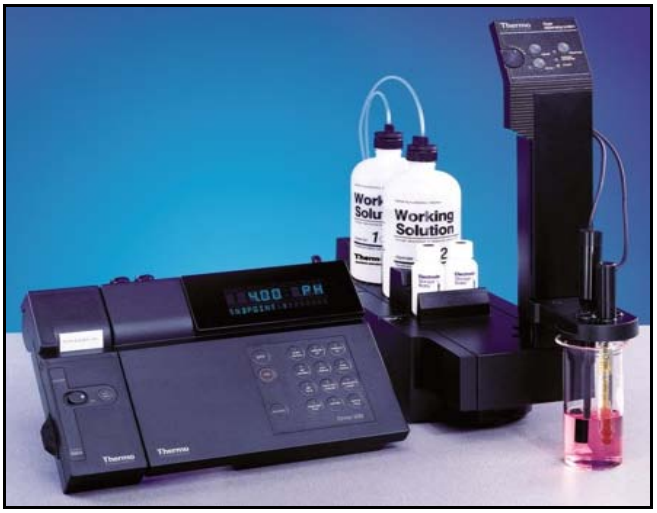

Fig. 21—Thermo scientific autotitrator.

The calcium concentration is measured using the atomic absorbance technique, with the AAnalyst 700 flame type. The equipment is shown in **Fig. 22**, and it is designed and assembled by Perkin Elmer.

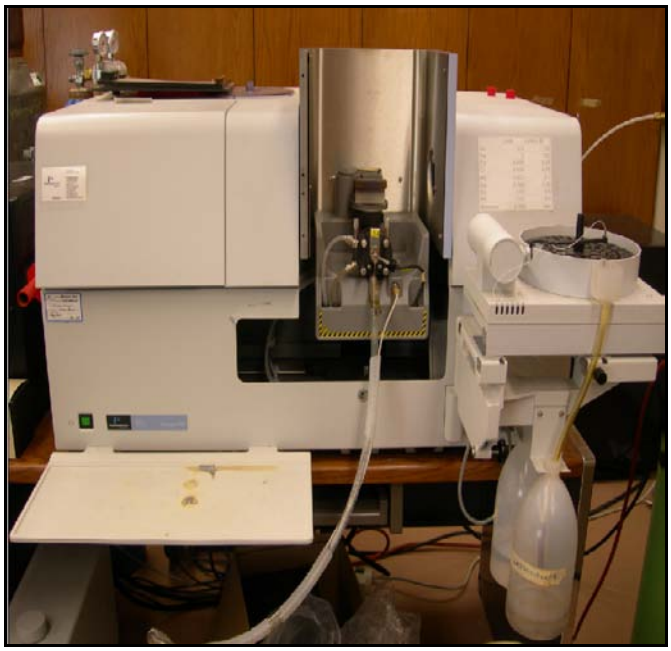

Fig. 22—AAnalyst 700 flame type.

CHAPTER V

RESULTS AND ANALYSIS

5.1 Perforating of Indiana Limestone Core Samples

This research project is based on seventeen experiments, but due to the fracturing of the initial core samples, just six experiments are reported and analyzed in detail. The first five core samples were Indiana limestone, and they were perforated using 15 gram charges. Long fractures were created due to the stress generated by the charge penetrating the rock. It was decided to continue and run the core flood experiments with these cores, to determine whether these fractures would significantly affect the results or not. The fractures observed in these five core samples trigger the collapse of the cores during the core flood experiments, and they highly affected the results (**Fig. 23 and 24**). The flow performance of the core samples was not dominated by the permeability of the core itself and the perforation tunnels efficiency, the flow performance was highly affected by the fractures as well.

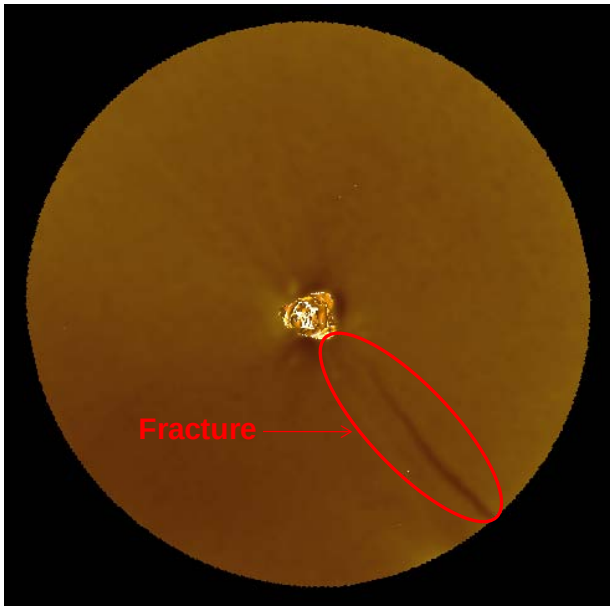

Fig. 23—Inlet face of a perforated Indiana limestone core sample.

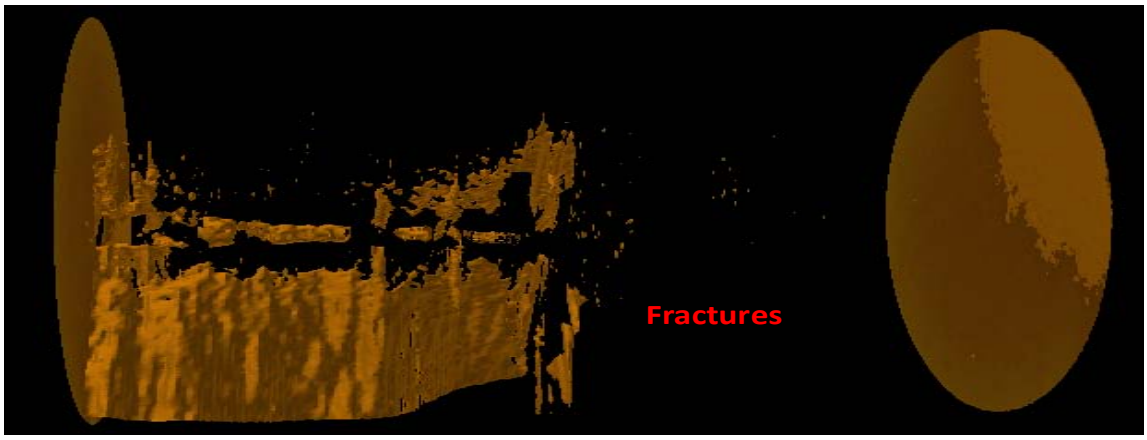

Fig. 24—3D Image of a perforated Indiana limestone core sample.

The flow path of the acid (wormholes) was highly dominated by the fractures. Due to the high conductivity of the fractures, acid flowed through the fractures rather than through the perforation tunnels (**Fig. 25**). Thus it was not possible to compare and evaluate the results obtained from these five experiments. **Table 1** shows the results obtained from these five cores. It can be observed that there is not a clear tendency in the relation between injectivity and the type of charge used. Since the cores have similar rock properties, it is expected to observe similar results and a clear trend in the relation between injectivity and type of charge used.

Table 1—Indiana limestone cores perforated with 15 grams charges

Shot Type	Injection ΔP, psi	Acid to Break through, ml
Conventional	274.00	66.67
Reactive	327.00	58.23
Conventional	321.50	41.67
Reactive	660.00	101.67
Conventional	206.00	62.5

In order to try to avoid the fracturing of the cores, four Indiana limestone cores were perforated with 7 gram charges rather than with 15 gram charges. Since this type of rock is highly brittle, these core samples were fractured as well during the shooting of the charges. The fractures significantly affected the results such as injectivity and volume of acid to breakthrough. It was observed that acid flowed through the fractures

as well. **Table 2** shows a summary of the results obtained from this set of core samples. Higher injectivity was observed in the cores perforated with reactive charges, but as mentioned before; these results are meaningless because the flow performance and acid flow path are highly dominated by the fractures.

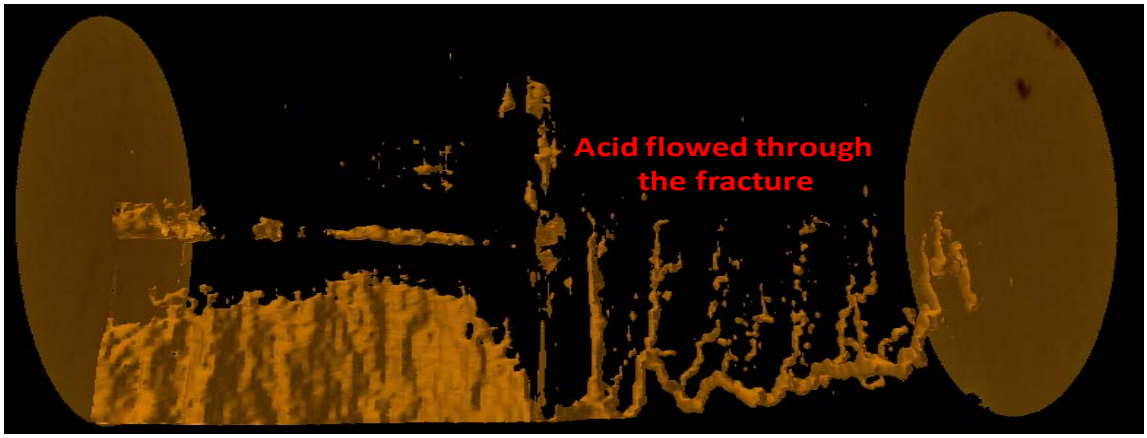

Fig. 25—3D Image of an Indiana limestone core sample after acidizing.

Table 2—Indiana limestone cores perforated with 7 grams charges

Shot Type	Injection ΔP, psi	Acid to Break through, ml
Conventional	406.00	65
Reactive	371.00	60
Conventional	421.00	64.17
Reactive	386.00	73.33
Conventional	953.00	77.5
Reactive	335.00	60.42

Since the fracturing of the cores was not allowing the comparison of the results, it was decided to perforate a set of cream chalk cores. This type of rock is softer than the Indiana limestone type, thus it was expected to avoid the fracturing of the core samples. The results obtained are reported and analyzed in detail in the following sections.

5.2 Perforating of Cream Chalk Core Samples

As discussed in the previous section, cream chalk cores were used for the last set of experiments to try to mitigate the fracturing of the cores. Six experiments were run using

different charges and pressure conditions. **Table 3** shows a summary of the perforating results obtained.

Table 3—Perforating results

Test Number	Type of Shaped Charge	Perforating Pressure Condition	Inlet Perforation Diameter, inches	Perforation Length, inches	Volume of Perforation, cubic inches
Core 1	Conventional	Balanced	0.206	10.27	0.33
Core 2	Reactive	Balanced	0.257	10.39	0.49
Core 3	Conventional	Overbalanced	0.229	10.27	0.32
Core 4	Reactive	Overbalanced	0.263	10.51	0.50
Core 5	Conventional	Balanced	0.320	17.72	1.09
Core 6	Reactive	Balanced	0.390	15.42	1.05

The first two samples of this set of cores were perforated at a balanced pressure condition, meaning that the pore pressure and simulated wellbore pressure were equal (3,000 psi) before the detonation of the 7 gram charges. **Fig. 26** shows the core perforated with a conventional charge (core 1) and **Fig. 27** shows the core perforated with a reactive charge (core 2). The presence of liner debris in both cores was observed, but there is not a method to accurately estimate the amount of debris from the CT scan images. Fractures were observed at the tip of the perforation tunnels in both cores, but the fractures are considerably longer in core 2. **Fig. 28** shows a comparison of the fractures at the tunnels' tip between core 1 and 2. This observation confirms the fact that the increase in pressure generated by the exothermic reaction propagates the length of these fractures, which are originally created by the liner penetrating the rock. The diameter of the perforation and the tunnel's length were observed to be larger in core 2, which resulted in a larger perforation tunnel's volume. Since both shaped charges have exactly the same dimensions, this observation verifies that some of the crushed rock is expelled into the simulated wellbore.

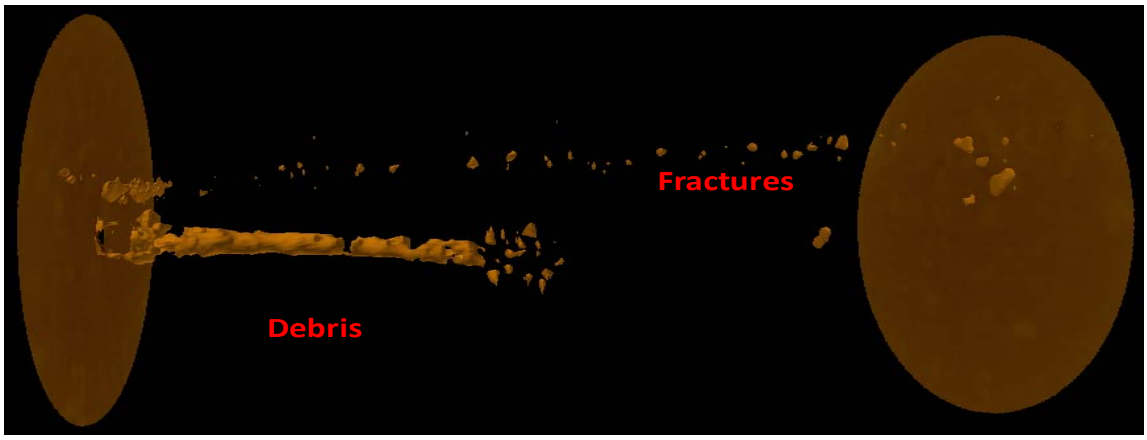

Fig. 26—3D Image of Core 1.

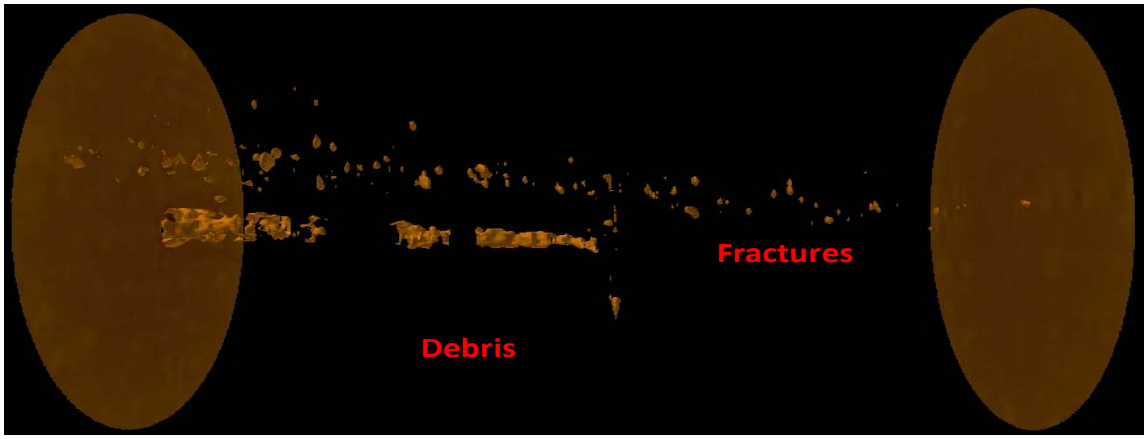

Fig. 27—3D Image of Core 2.

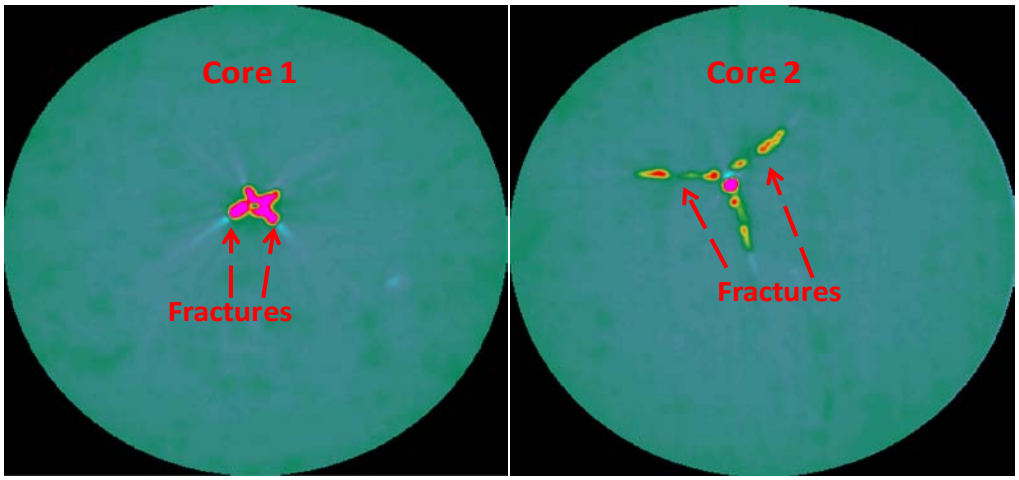

Fig. 28—Comparison of the fractures at the tip of the perforations.

Cores 3 and 4 were perforated using 7 gram charges as well, but they were perforated at an overbalanced condition with a 500 psi overbalanced pressure. **Fig. 29 and 30** show the CT scan images of these two cores. The results are very similar to the first two cores. Debris are observed in both cores, the fractures at the tip of the tunnels are longer in core 4, and the volume of the perforation tunnel in core 4 is larger as well.

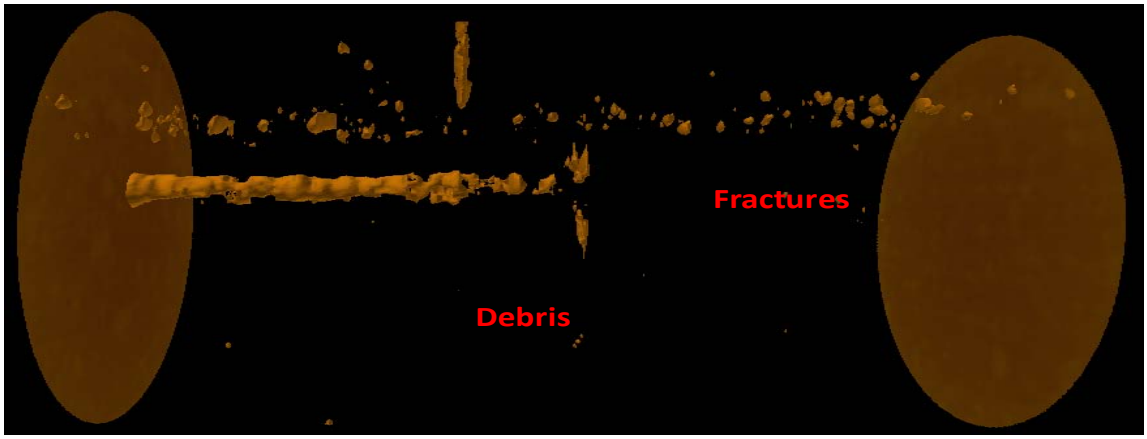

Fig. 29—3D Image of Core 3 test.

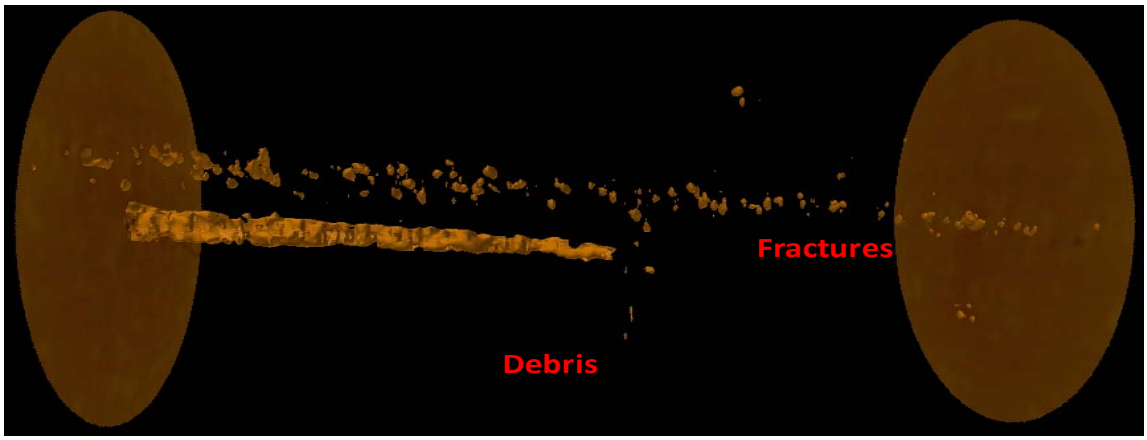

Fig. 30—3D Image of Core 4 test.

Cores 5 and 6 were perforated at a balanced pressure condition but using 12 gram charges (**Figs. 31 and 32**). The results are very similar to the previews cores, but core 5 which was perforated with a conventional charge has a much longer perforation tunnel, this perforation tunnel is 2.3 inches longer than the perforation in the core perforated

with a reactive charge (core 6). Since both cores were perforated using charges with the same explosive load, it is believed that this significant difference in perforation length is due to variations in the core samples.

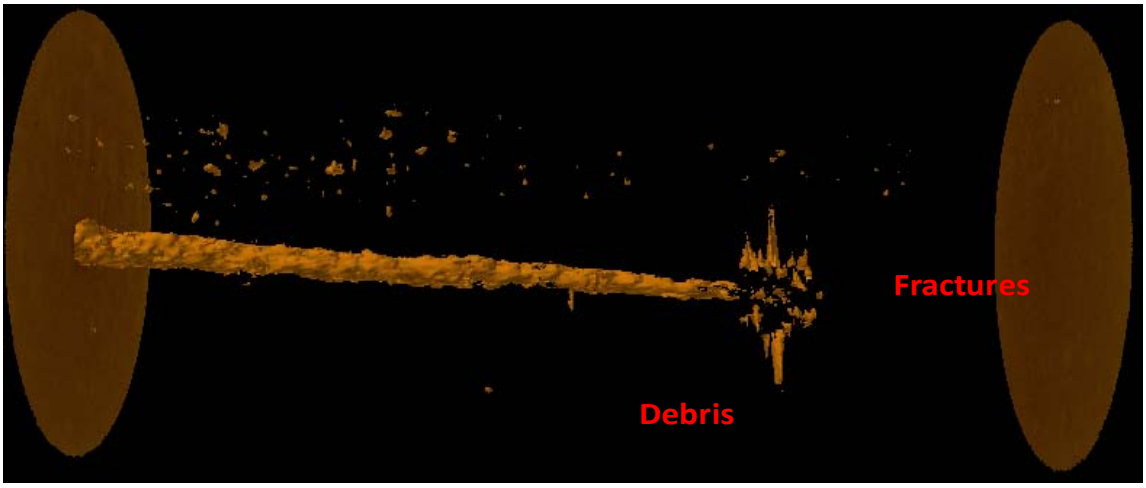

Fig. 31—3D Image of Core 5 test.

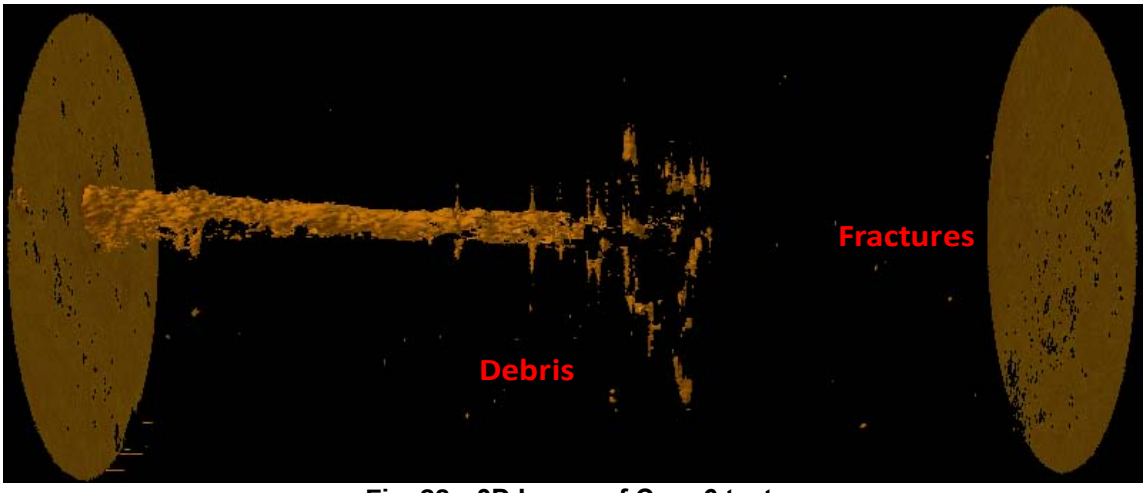

Fig. 32—3D Image of Core 6 test.

5.3 Core Flood Experiments

After evaluating the initial images of the perforated cores before acidizing, the core flood experiments were carried out. **Table 4** shows a summary of the results obtained. It can be observed that even though vugs were noticed in the CT images, the initial rock properties such as permeability and porosity are similar; this allows the

comparison of the results. As mentioned before, oil is first pumped at 10 cm^3/min until steady state flow is reached to evaluate the injectivity of the core samples. Comparing the first two experiments (cores 1 and 2), it can be noticed that even though core 1 has a higher initial permeability, the injection pressure in the core 2 test is lower, which means that the reactive charge (core 2) provided a more efficient and cleaner perforation tunnel. As reported by Bartko et al. (2007), higher injectivity would help to propagate more dominant wormholes. This observation was also noticed in our experiments. **Figs. 33 and 34** show the 3D CT images of these cores, it can be observed that the core perforated with a reactive charge (core 2) provided more dominant wormholes, which resulted in less acid to breakthrough.

Table 4—Core flood experiments' results

Test Number	Original Rock Permeability, md	Porosity, fraction	Injection ΔP, psi	Acid to Break through, ml	Acid to Break through, PV
Core 1	5.29	0.257	375	95	0.1851
Core 2	3.48	0.256	351	91	0.1802
Core 3	2.67	0.254	365	87	0.1712
Core 4	2.89	0.256	298	85	0.1706
Core 5	3.95	0.259	224	56	0.4605
Core 6	2.58	0.258	288	63	0.2589

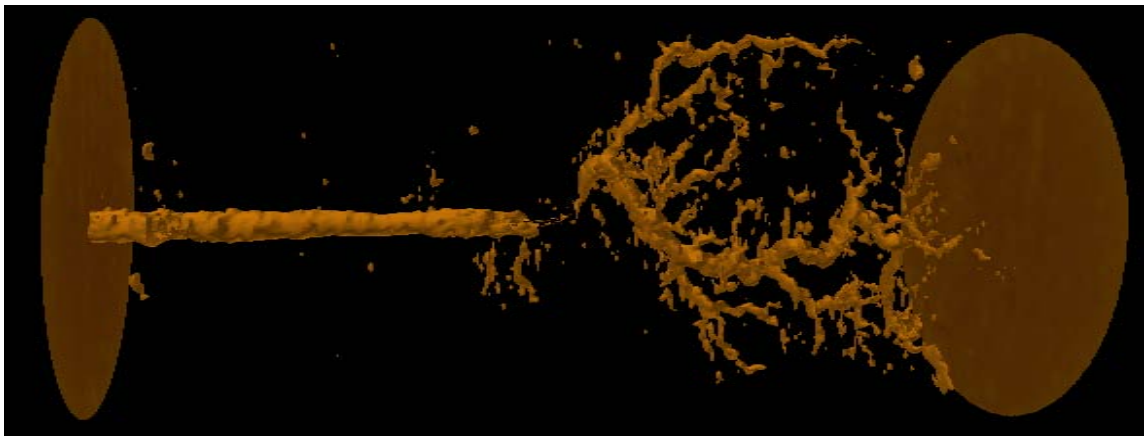

Fig. 33—3D Image of Core 1 test after acidizing.

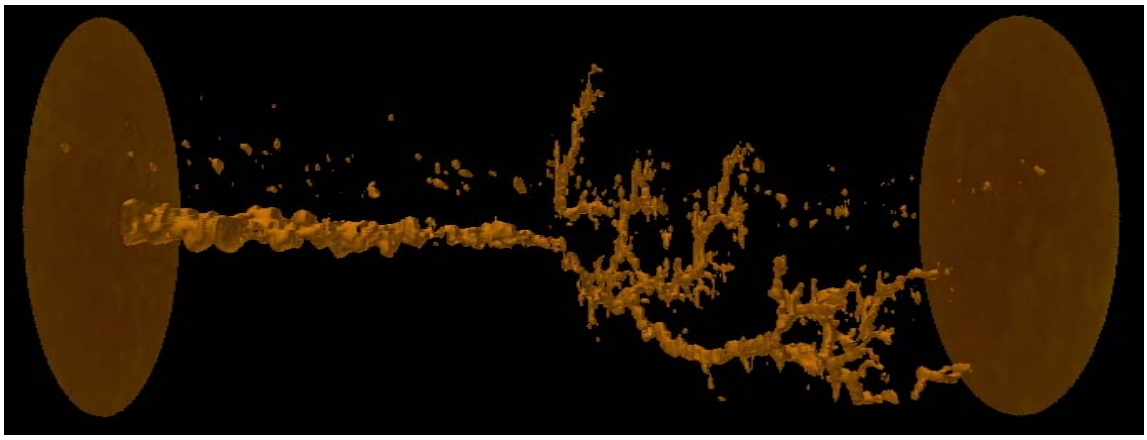

Fig. 34—3D Image of Core 2 test after acidizing.

The initial rock permeability of the cores 3 and 4 are very similar, but core 4 which was perforated with a reactive charge showed higher injectivity. **Figs. 35 and 36** show the CT images of the cores after acidizing. The results of these two cores are consistent with the results obtained from cores 1 and 2, since less acid was needed to breakthrough core 4. As can be noticed in Fig. 36, core 4 collapsed at the tip of the perforation during the core flood experiment, this was triggered by the long fractures observed at the tip of the perforation tunnel before acidizing.

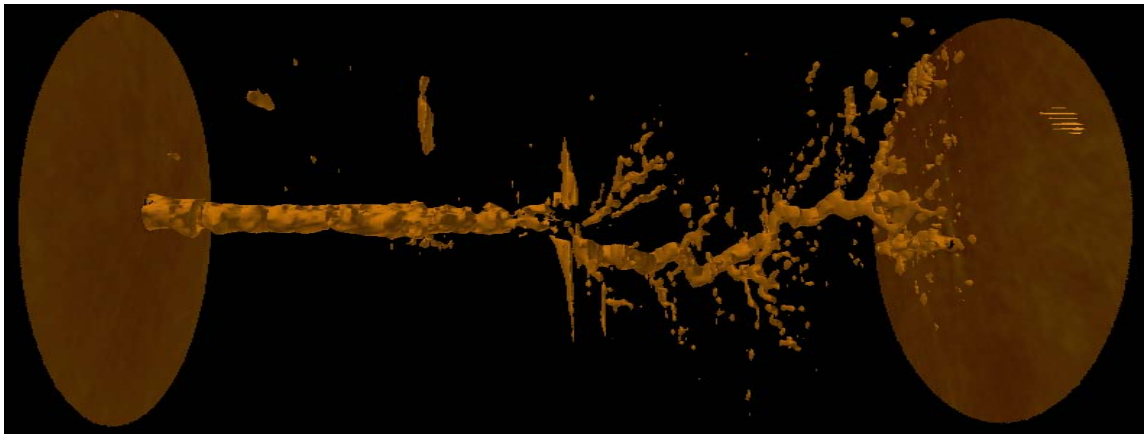

Fig. 35—3D Image of Core 3 test after acidizing.

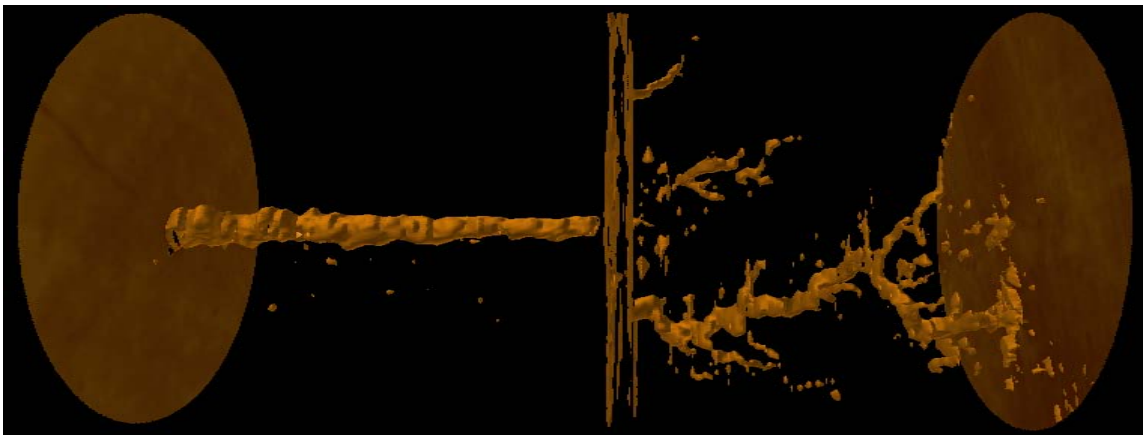

Fig. 36—3D Image of Core 4 test after acidizing.

The results obtained from cores 5 and 6 (**Figs. 37 and 38**) do not provide any further information in terms of the relation between injectivity and acid volume to break through, because the perforation tunnels' lengths are considerably different. But it can be observed that the acid pore volume needed to break through core 6 is significantly lower that the pore volume needed in core 5, meaning that wormholes propagation was more efficient in the core perforated with the reactive charge. It is important to remember that the term "acid pore volume to break through" is the ratio of the acid volume used to break through, over the pore volume from the tip of the perforation to the outlet. It can also be observed that the difference in pore volume to break through is more evident or significant in these two cores than in the previous experiments.

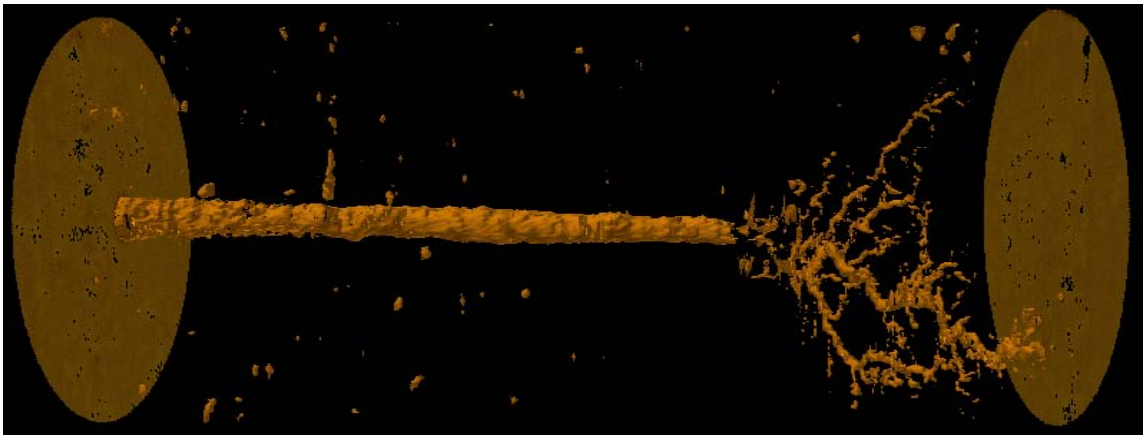

Fig. 37—3D Image of Core 5 test after acidizing.

It is believed that the explanation for the results obtained from the last two experiments is that these cores were perforated with bigger charges (12 gram charges), meaning that the reactive charge had more reactive materials to clean the perforation than in the previous experiments where 7 gram charges were used.

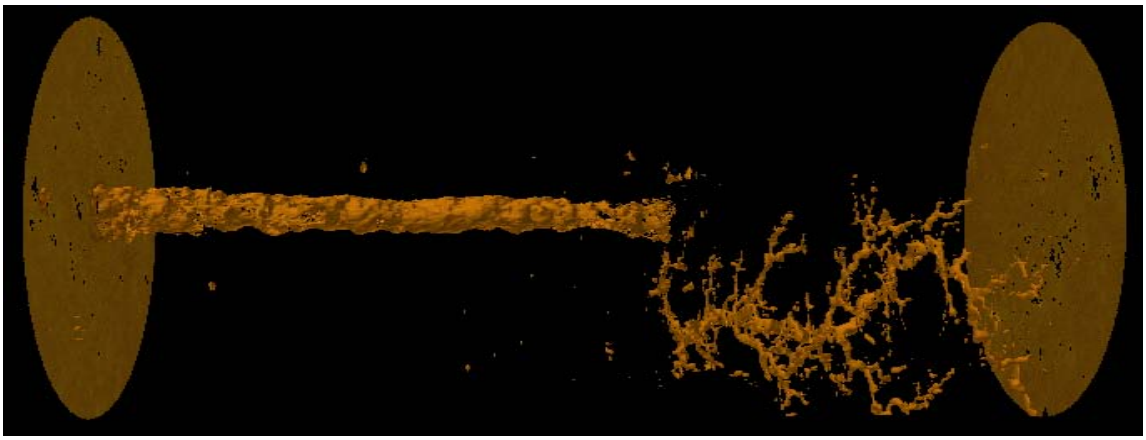

Fig. 38—3D Image of Core 6 test after acidizing.

Fig. 39 shows the results obtained from the compositional analysis of the fluid samples collected in core 1 test. It can be observed that acid behaves like a piston displacing the oil in the core. This event is confirmed by the samples showed in **Fig. 40,** since acid is observed coming out of the system after it breaks through the core (sample 9). This data was then correlated with the pressure data to confirm the exact time that acid breaks through the core, which was used to estimate the acid volume needed to break through. The results obtained in the rest of the experiments are very similar to the results from core 1 test, thus they are not reported.

Fig. 41 shows the fluid samples collected during the flow back of core 1 test. It can be observed that there is not debris present in these samples, meaning that debris is removed from the perforations by the acid. This samples didn't provide any further information, thus the flow back samples collected from the rest of the experiments are not reported, since the results are the same.

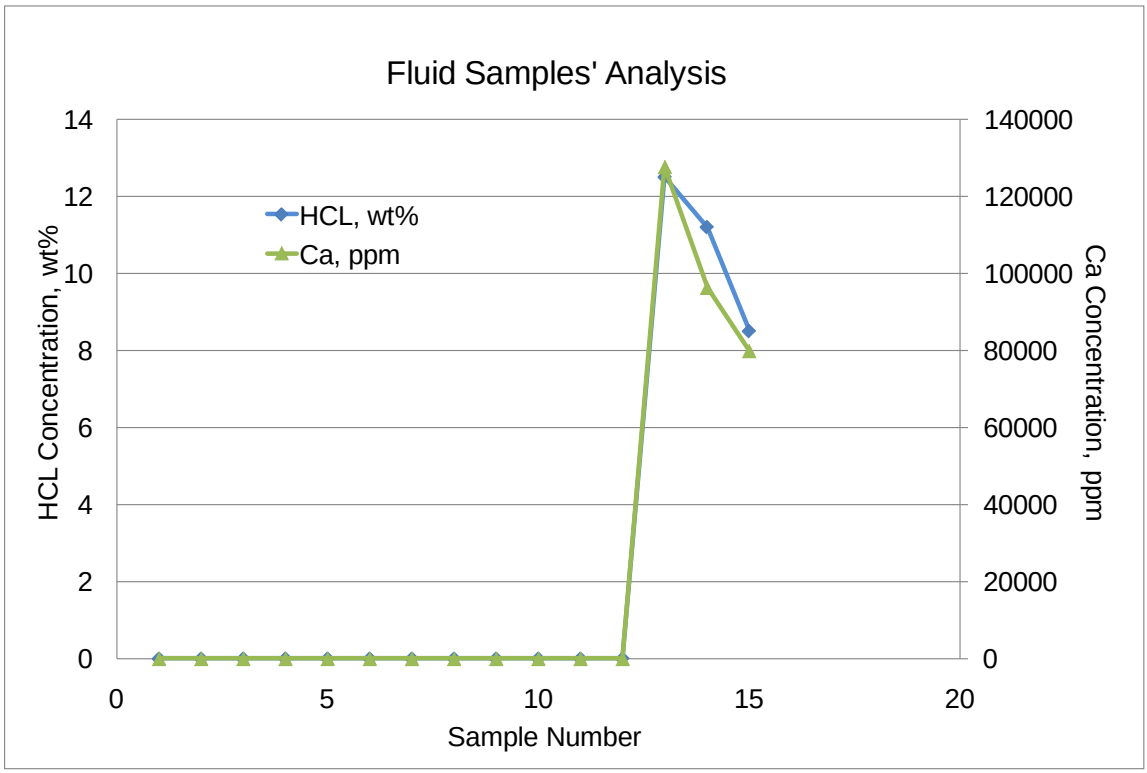

Fig. 39—HCL and Ca concentration Core 1 test.

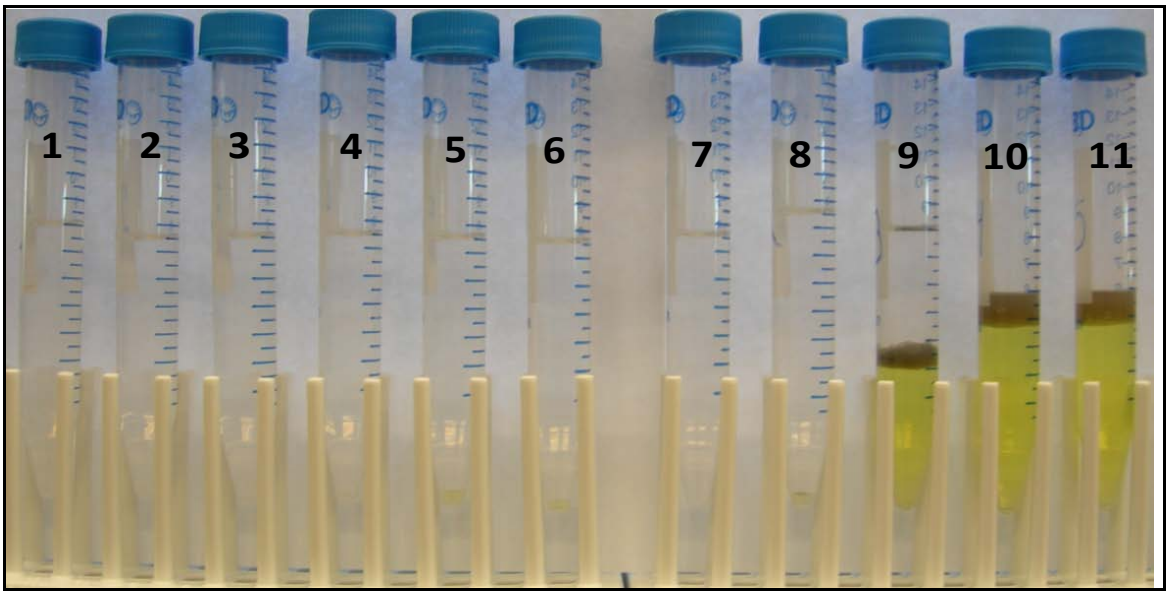

Fig. 40—Picture of fluid samples obtained in Core 1 test.

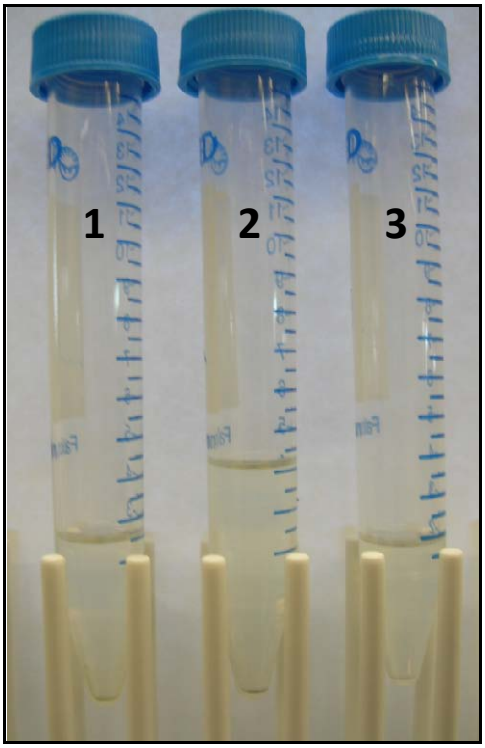

Fig. 41—Picture of flow back fluid samples obtained in Core 1 test.

To sum up, it can be said that perforation tunnels obtained with reactive charges showed higher injectivity, this fact was confirmed by the results obtained in terms of acid pore volume to breakthrough. As mentioned before in the acidizing fundamentals section, wormholes propagation is dependent on the acid flux (Fig. 7). Thus it is believed that reactive charges provide cleaner perforations, which increases the acid flux at the tip of the perforation and at the same time helping to propagate wormholes more efficiently.

CHAPTER VI

CONCLUSIONS AND RECOMMENDATIONS

6.1 Conclusions

After finalizing this research work and observing the results obtained from the perforated cores and core flood experiments, the resulting conclusions are:

- Reactive charges offer perforation tunnels with higher injectivity. Higher injectivity perforations would be an important advantage for stimulation jobs, flow performance, and well productivity.
- The CT scan images and effluent fluid samples confirmed the presence of debris in the cores perforated with conventional and reactive charges. It was not possible to quantify the amount of debris in the perforations, thus further research should be carried out to measure the concentration of the liner's materials in the fluid samples. This step would provide a better estimation of the cleaning efficiency obtained when perforating with reactive charges.
- The increase in injectivity provided by the reactive charges results from the cleaning and fractures created at the tip of the perforations. Even though liner's debris is still observed in the cores perforated with reactive charges, it is believed that this technology is capable of cleaning the perforations more efficiently than conventional charges, regardless of the pressure condition used for the detonation. First, because higher injectivity was observed in the cores perforated with reactive charges, and also because an increase in the perforations diameter was noticed, which confirms that some of the crushed rock is expelled into the simulated wellbore.
- As noticed from the results obtained in the core flood experiments, higher injectivity tunnels help to propagate more dominant and straighter wormholes. This reduces the volume of acid needed to reach a certain distance into the core sample or formation. But further research should be carried out to determine if the difference in acid volume to break through observed in this experimental

work, would really have an economic impact or help to obtain a smaller post treatment skin factor.

6.2 Recommendations for Future Work

Even though this research project offers a clear evaluation of the effect of conventional and reactive charges on acid wormholing, further research should be carried out to have a better understanding and estimation of certain factors, such as:

- The cleaning efficiency provided by the reactive charges should be better estimated by measuring the amount of liner's materials in the effluent fluid samples.
- As mentioned before, this study was carried out with 4 inches in diameter and 20 inches long cores, but larger cores should be used to better avoid the fracturing of the cores during the detonation of the charges and during the core flood experiments. This would also help to better simulate the actual field conditions by using more representative cores.
- Since there is a wide variety of carbonate rock types, different types of carbonate rocks should be used to confirm if the results obtained in this study would be consistent with different types of formations.
- It would be of great advantage to perform the perforating and acidizing of the cores in the same apparatus, first to avoid the handling and movement of the cores from one set up to another, and also to better simulate the real field conditions.

REFERENCES

Allen, T. O. and Worzel, H. C., "Productivity Method of Evaluating Gun Perforating", Spring Meeting of the Southwestern District, Fort Worth, Texas, March 1956.

Bartko, K.M., Chang, F.F., Behrmann, L.A., and Walton, I.C.: "Effective Matrix Acidizing in Carbonate Reservoir-Does Perforating Matter?", paper SPE 105022, presented at the 2007 15th SPE Middle East Oil and Gas Show, Bahrain, 11-14 March.

Bell, M.R.G., Hardesty, J.T., Clark, N.G.: "Reactive Perforating: Conventional and Unconventional Applications, Learnings and Opportunities", paper SPE 122174, presented at the 2009 SPE European Formation Damage Conference, Scheveningen, The Netherlands, 27-29 May.

Bell, W., Brieger, E. and Harrigan, J., "Laboratory Flow Characteristics of Gun Perforations", paper SPE 3444, presented at the 1971 46th SPE Annual Fall Meeting, New Orleans, 3-6 October.

Bell, W. T., Sukup, R. A. and Tariq, S. M., *Perforating*, SPE Monograph, 1995.

Economides, Michael J. Hill, A. Daniel. and Economides, Christine E. 1994. *Petroleum Production Systems*, first edition. Upper Saddle River, New Jersey: Prentice Hall.

Handren, P.J., T.B. Jupp, and J.M. Dees, Oryx Energy Co., "Overbalance Perforating and Stimulation Method for Wells", paper SPE 26515, presented at the 1993 68th Annual Technical Conference and Exhibition of the Society of Petroleum Engineers, Houston, Texas, 3-6 October.

Wang, Y., Hill, A.D., and Schechter, R.S., "The Optimum Injection Rate for Matrix Acidizing of Carbonate Formations", paper SPE 26578, presented at the 1993 68th Annual Technical Conference and Exhibition of the Society of Petroleum Engineers, Houston, Texas, 3-6 October.

Williams, Bert B. Gidley, John L. and Schechter, Robert S. 1979. *Acidizing Fundamentals*, SPE monograph volume 6. Dallas, Texas: Millet the Printer, Inc.

VITA

Name: Nerwing Jose Diaz

Address: 3116 TAMU - 714 Richardson Building College Station, Tx.77843

Email Address: nerwingdiaz@hotmail.com

Education: M.S. Petroleum Engineering. Texas A&M University, Texas. 2010
B.S. Industrial Engineering. Rafael Belloso Chacin University, Venezuela. 2006

Employment History: Baker Hughes-INTEQ, Current

Baker Hughes-Centrilift, 2005-2006

This thesis was typed by the author.